Published December 1, 1996

The Effect of Hyperosmolality on the Rate of Heat Production of Quiescent Trabeculae Isolated from the Rat Heart

D.S. LOISELLE,‡ G.J.M. STIENEN,* C. VAN HARDEVELD,* E.T. VAN DER MEULEN,* G.I. ZAHALAK,§ J. DAUT,‖ and G. ELZINGA*

From the *Laboratorium voor Fysiologie, Vrije Universiteit, 1081 BT Amsterdam; ‡Department of Physiology, School of Medicine, University of Auckland, Auckland 1030, New Zealand; §Department of Mechanical Engineering, Washington University, St Louis, Missouri 63130; and ‖Institut für Normale und Pathologische Physiologie, Universität Marburg, 35033 Marburg, Germany

ABSTRACT We have measured the rate of heat production of isolated, quiescent, right ventricular trabeculae of the rat under isosmotic and hyperosmotic conditions, using a microcalorimetric technique. In parallel experiments, we measured force production and intracellular calcium concentration ($[Ca^{2+}]_i$). The rate of resting heat production under isosmotic conditions (mean ± SEM, $n = 32$) was 100 ± 7 mW (g dry wt)$^{-1}$; it increased sigmoidally with osmolality, reaching a peak that was about four times the isosmotic value at about twice normal osmotic pressure. The hyperosmotic thermal response was: (*a*) abolished by anoxia, (*b*) attenuated by procaine, (*c*) insensitive to verapamil, ouabain, and external calcium concentration, and (*d*) absent in chemically skinned trabeculae bathed in low-Ca^{2+} "relaxing solution." Active force production was inhibited at all osmolalities above isosmotic. Passive (tonic) force increased to, at most, 15% of the peak active force developed under isosmotic conditions while $[Ca^{2+}]_i$ increased, at most, 30% above its isosmotic value. We infer that hyperosmotic stimulation of resting cardiac heat production reflects, in large part, greatly increased activity of the sarcoplasmic reticular Ca^{2+} ATPase in the face of increased efflux via a procaine-inhibitable Ca^{2+}-release channel.

KEY WORDS: hypertonicity • cardiac basal metabolism • chemical skinning • intracellular calcium • procaine

INTRODUCTION

It has been known since early this century that hyperosmolality depresses the active force production of skeletal (Overton, 1902; Demoor and Philippson, 1908) and smooth (Dale, 1913) muscle. Comparable depressive effects on cardiac muscle were revealed mid-century (Hirvonen, 1955). These have subsequently been confirmed in a variety of species and preparations including trabeculae (Chapman, 1978; Kawata et al., 1983), papillary muscles (Koch-Weser, 1963; Hermsmeyer et al., 1972), isolated atria (Little and Sleator, 1969; Beyer et al., 1986) and whole-hearts both in vitro (Ben-Haim et al., 1992*b*) and in situ (Sperelakis et al., 1960). Contractile depression occurs in the face of undiminished Ca^{2+} transients (Allen and Smith, 1987).

In quiescent cardiac preparations, hyperosmotic challenge induces transient contractures (Hermsmeyer et al., 1972; Kawata and Kawagoe, 1975; Lado et al., 1984; Ohba, 1984). In skeletal muscle, transient contractures and depression of active force development are associated with increased stiffness (Lännergren, 1971; Månsson, 1994), decreased contractile velocity (Edman and Hwang, 1977; Gulati and Babu, 1984; Ford et al., 1991), and suppression of actomyosin ATPase activity (Krasner and Maughan, 1984; Zhao and Kawai, 1993).

Address correspondence to D.S. Loiselle, Department of Physiology, School of Medicine, University of Auckland, Auckland, New Zealand. Fax: 64-9-373-7499; E-mail: ds.loiselle@auckland.ac.nz

These depressive effects on mechanical function are accompanied by a paradoxical enhancement of resting metabolic activity. Hypertonicity enhances the rates of heat production (Hill, 1968; Yamada, 1970; Chinet and Giovannini, 1989; Chinet, 1993), O_2 consumption (Sekine et al., 1957), CO_2 production (Kuzuya et al., 1965), glucose uptake (Clausen et al., 1970), glycogenolysis (Clausen, 1968), lactate formation (Daemers-Lambert et al., 1966; Clausen, 1968), and phosphocreatine breakdown (Daemers-Lambert et al., 1966; Homsher et al., 1974; Rapoport et al., 1982) of various skeletal muscle preparations.

Recently, the potentiating effect of hyperosmolality on the rate of oxygen consumption of the perfused, arrested whole heart has been reported (Hanley et al., 1994*a*). In that study, hyperosmotic perfusion increased the rate of oxygen consumption of the arrested heart profoundly while effecting only a modest increment of passive (diastolic) pressure. These apparently conflicting results were reconciled by proposing that hyperosmotic perfusion induces release of Ca^{2+} from the sarcoplasmic reticulum, thereby greatly potentiating the activity (and metabolic cost) of its Ca^{2+} pump.

The present study was designed to confirm and extend those observations. In order to avoid the possibility that some portion of the oxidative response observed in the perfused whole heart (Hanley et al., 1994*a*) reflected greatly increased metabolic activity of its coronary vascular smooth muscle, we opted to use a nonper-

Published December 1, 1996

fused preparation. To obviate the uncertainty associated with inferring passive wall tension from measurement of diastolic pressure, we sought a preparation in which cardiac myocytes are arranged uniaxially. The preparation had to be small enough to ensure adequate oxygenation in the face of elevated energy expenditure yet large enough to permit accurate measurement of both passive and active force development. In addition, it had to allow estimation of changes in intracellular calcium ion concentration. These various requirements were met by use of the isolated, superfused, rat ventricular trabecula—a preparation that differs in size from the perfused whole heart by several orders of magnitude. We chose a measurement technique, namely microcalorimetry, the biophysical basis of which is unrelated to the measurement of oxygen consumption. As a result, we present the first report of the thermal consequences of elevated osmolality in isolated, quiescent, cardiac muscle.

MATERIALS AND METHODS

Calorimetry

Intact preparations. Male rats, weighing 190–420 g, were killed by cervical dislocation, and the heart was quickly excised. Trabeculae (or, occasionally, papillary muscles) of length 1.25–3.1 mm and dry weight 4.3–50.8 μg were dissected from the right ventricle and immediately transferred to the holding chamber of the calorimeter. A suitable preparation was tied at each end with a single loop of 25 μm (10/0 USP) nylon thread which was, in turn, tied to one of the stimulating electrodes. In later experiments, some preparations were attached to the stimulating electrodes directly by small aluminum clips. By turning a pair of micromanipulators connected to the electrodes, the muscle was advanced into the measurement chamber.

At the conclusion of the experiment, the muscle was returned to the holding chamber where its dimensions were determined under ×40 magnification. The threads were severed, and the dry weight of the preparation was determined using a Model 29 CAHN (Cahn Instruments, Inc., Cettitos, CA) electro-balance.

Skinned preparations. In three experiments, trabeculae were chemically skinned by immersion in relaxing solution (see below) supplemented with 1% (vol/vol) Triton X-100 for a minimum of 30 min. They were then transferred to the calorimeter and subsequently studied in the usual manner except that osmotic compression was achieved by the addition of various concentrations of polyvinylpyrrolidone (PVP)[1].

Solutions. Dissection was performed in a solution of the following composition (mmol l^{-1}): NaCl 60, K_2SO_4 60, $CaCl_2$ 1, $MgSO_4$ 3, sodium pyruvate 2, glucose 20, HEPES 10. The pH was adjusted to 6.8 by addition of Tris. Experiments were performed in a Tyrode solution the standard (isosmolar) composition of which was: NaCl 144, KCl 6, $CaCl_2$ 2, $MgSO_4$ 1, Na_2HPO_4 1, sodium pyruvate 2, glucose 20, HEPES 10. The pH was adjusted to 7.4 by addition of Tris. The solution was bubbled with 100% O_2 at 37°C. An isosmotic-high-K^+ solution was achieved by substitution of KCl for NaCl.

Hyperosmotic solutions were made by addition of sucrose, mannitol, NaCl, or KCl to the standard isosmotic solution. (We thus distinguish between isosmotic-high-K^+ and hyperosmotic-high-K^+ solutions.) The osmolality of selected solutions was measured using a Wescor 5500 Vapor Pressure Osmometer (Wescor Inc., Logan, Utah) with the following results (mosmol $liter^{-1}$): isosmotic Tyrode without metabolic substrates 280, isosmotic Tyrode (i.e., with metabolic substrates) 300, Tyrode + 150 mmol $liter^{-1}$ NaCl 573, Tyrode + 300 mmol $liter^{-1}$ mannitol 587, Tyrode + 300 mmol $liter^{-1}$ sucrose 613. The osmolality of other hyperosmotic solutions was calculated by assuming osmotic coefficients of 1.0 for sucrose and mannitol and of 2.0 for NaCl and KCl, independent of concentration.

For skinned trabeculae, the standard "relaxing" solution was as follows (mmol l^{-1}): $MgCl_2$ 10.6, Na_2ATP 5.3, EGTA 20, K-propionate 35.4, phosphocreatine (PCr) 10, MgATP 5, and creatine kinase 0.4 mg ml^{-1} (350 U mg^{-1} at 25°C). Hyperosmotic conditions were mimicked by the addition of 5, 10, and 15 g dl^{-1} PVP. The "activating" solution contained (mmol $liter^{-1}$): $MgCl_2$ 8.6, Na_2ATP 5.3, CaEGTA 20, K-propionate 37.7, PCr 10, and creatine kinase 0.4 mg $mliter^{-1}$. All solutions contained 100 mmol $liter^{-1}$ BES (2-[bis(2-hydroxyethyl)amino]ethanesulfonic acid) and were adjusted to pH 7.1 using KOH. Ionic strength (adjusted using K-propionate) was 200 mmol $liter^{-1}$.

The calorimeter: Principle of operation. The calorimeter has been described in detail elsewhere (Daut and Elzinga, 1988). Briefly, it consists of a Perspex tube, of inside diameter 800 μm, into the walls of which have been embedded two hexagonal arrays of chromel-constantan thermocouples separated by a distance of 4 mm (Fig. 1 *A*). Using the micromanipulators, the center of the trabecula is located midway between the thermocouple arrays (corresponding to location *0* in Fig. 1 *B*). As soon as a flow of bathing solution through the tube is commenced, the downstream thermocouples experience a rise of temperature the extent of which is proportional to the rate of production of heat by the trabecula. Absolute rates of heat production are calculated with respect to a baseline established by manipulating the preparation 5 mm downstream, i.e., 3 mm below the downstream thermocouples. Flow, at a rate of 1 μl s^{-1}, is provided by a reciprocating pump (Labomatic MDP 16; Reichelt Chemie Technik, Heidelberg, Germany). The output of the thermocouples is amplified by a custom-built, low-noise differential amplifier, passed through a low-pass filter (−3 dB point of 1 Hz) and displayed on a chart recorder (SE 120, BBC; Goerz Metrawatt; ABB Goerz AG, Vienna, Austria).

Calibration. The calorimeter was calibrated by advancing a thermistor into the measurement chamber and liberating known power at various locations between the arrays of thermocouples. Calibration curves (power output as a function of location) were determined independently, as a function of osmolality, for each osmotic species. Power output (for a fixed power input) varied with both geometric location and osmotic species (Fig. 1 *B*). Calibration results using distilled H_2O, isosmolar Tyrode (with and without oxygenation), twice standard osmolar NaCl, and 1.5 or 2 times standard osmolar sucrose solutions all fell within the standard error bars shown, through which a straight line has been fitted over the range from −1.0 to +1.5 mm. Since the longest trabecula placed in the calorimeter was 3.1 mm, it is appropriate to use the mean output shown at 0.0 mm as the value with which to convert any observed myothermic response to absolute units of μW when any of these osmotic conditions prevailed. But, as can also be seen in Fig. 1 *B*, when PVP was used (together with skinned trabeculae), then a different calibration value was required for each PVP concentration. This result raises the possibility that viscous heating may contaminate the output of the calorimeter.

Viscous heating. Viscous heating is the direct conversion into thermal energy of the mechanical work expended in deforming

[1] *Abbreviations used in this paper:* DNP, dinitrophenol; PVP, polyvinylpyrrolidone; R_{max}, ratio of fluorescence at 340 nm to that at 380 nm in the presence of saturating levels of Ca^{2+}; R_{min}, the fluorescence ratio in the absence of Ca^{2+}; SR, sarcoplasmic reticulum.

Published December 1, 1996

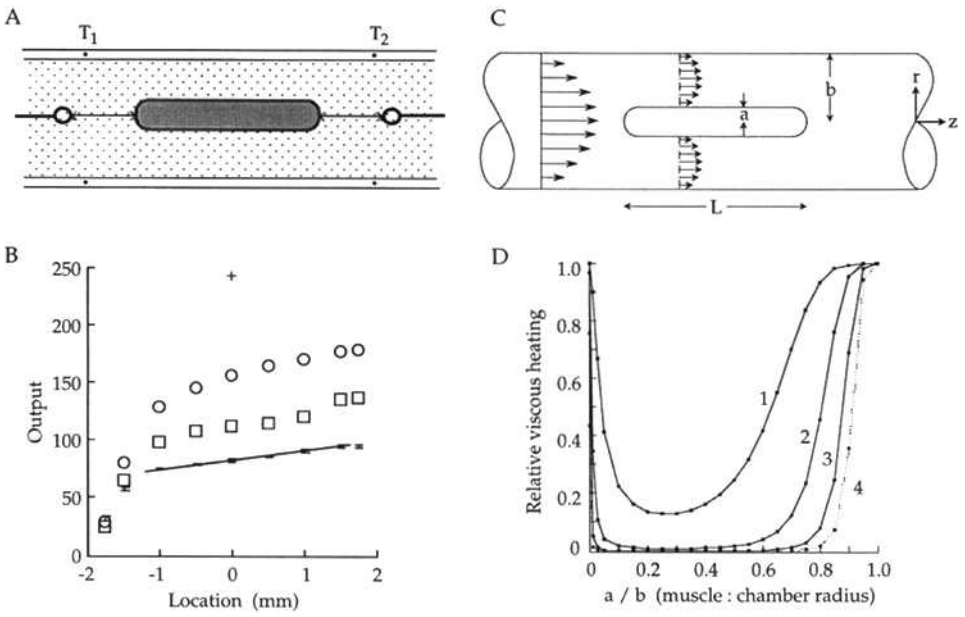

FIGURE 1. The calorimeter. (*A*) Schematic diagram of the measurement chamber. The muscle preparation is tied at either end to an electrode and advanced into the chamber to lie midway between two arrays of thermocouples (T_1 and T_2). At a fixed rate of flow, the difference in temperature between the downstream and upstream thermocouples ($T_2 - T_1$) is proportional to power generated by the muscle. (*B*) Calibration of the calorimeter as a function of geometric location and perfusion solution. A thermistor was advanced into the measurement chamber, to lie at the locations indicated, and current passed through it to dissipate power at a rate of 13.4 μW. Error bars show the mean ± SEM output response (in arbitrary units) using distilled H_2O, isosmotic Tyrode, and hyperosmotic NaCl or sucrose solutions. A straight line has been fitted through these data from −1.0 mm to +1.5 mm. (*open squares*) 5 g dl^{-1} PVP; (*open circles*) 10 g dl^{-1} PVP; (*cross*) 15 g dl^{-1} PVP. (*C*) Geometric model underlying assessment of viscous heating; *r* and *z*: radial and axial coordinates, *a*: radius of cylindrical muscle of length *L*, *b*: radius of calorimeter chamber; arrows indicate laminar flow profiles. (*D*) Ratio of viscous-to-total heat production, as a function of muscle-to-chamber radius (*a*/*b*), at a volume rate of flow of 1 μl s^{-1}, for various rates of myothermal heat production (labeled *1* to *4*, respectively): 0.6, 10, 100, and 400 mW (g dry weight)$^{-1}$.

the liquid that flows past the trabecula within the measurement chamber. The simplified model shown in Fig. 1 *C* is adopted in which the trabecula is represented by a circular cylinder, of radius *a* and length *L*, positioned coaxially with the cylindrical Perspex tube of diameter *b*. Bathing solution, which is assumed to be Newtonian, incompressible, and of viscosity η, is forced past the stationary, incompressible trabecula at a constant volumetric flow rate $\dot{V}$.

Both the velocity field and dissipation function for this simple annular flow are well known and lead to the following analytical expression for the rate of viscous heating per unit length (see APPENDIX for derivation):

$$\frac{\dot{H}_v}{L} = \frac{8\mu}{\pi b^4}\Psi(\zeta)\,\dot{V}^2, \qquad (1)$$

where $\zeta = b/a$ so that $\Psi(\zeta)$ is a dimensionless geometric factor.

Examination of Eq. 1 (which is the equivalent of Eq. A5, see APPENDIX) reveals that, even in the absence of a muscle, the downstream thermocouples experience a higher temperature than the upstream ones, the magnitude of which is given by solution of Eq. 1 with $\zeta^{-1} = 0$. In practice, the baseline for reference of subsequent myothermal heat production was defined as the output of the calorimeter in the absence of a muscle. With due account for this "correction," the relative contribution of viscous heating to the observed thermal output for muscles of various diameters and metabolic rates was calculated. The results are shown in Fig. 1 *D* where it can be seen that, as the gap between the muscle and the wall of the Perspex tube decreases (i.e., as $a \rightarrow b$), then the viscous component dominates the observed rate of heat production. As muscle radius, *a*, approaches zero, viscous heating again dominates, reflecting the fact that muscle heat production per unit length varies as a^2 whereas viscous heating (at a fixed rate of flow, $\dot{V}$) varies as $[\ln^{-1}(b/a)]$. Note that this is the excess viscous heating, above that measured in the absence of a trabecula.

In Fig. 1 *D*, the values of 100 and 400 mW (g dry wt)$^{-1}$ correspond approximately to the mean isosmotic and hyperosmotic rates of resting heat production, respectively, observed for rat right-ventricular trabeculae in the current study. The value of 0.6 μW (g dry wt)$^{-1}$ corresponds to that of resting amphibian skeletal muscle at 0°C (Hill, 1965). The values of $\dot{V}$, *b*, and η were 1 μl s^{-1}, 0.4 mm, and 1 cpoise ≡ 1 mN s m^{-2} (appropriate for H_2O), respectively; no variation of viscosity with temperature, salinity, or osmolality was assumed. Since no trabecula in the current study had a diameter >250 μm (i.e., $a/b \leq 0.625$), the contribution of viscous heating, even under isosmotic conditions, was probably negligible. Nevertheless caution is demanded. Since the viscosity of liquids varies inversely with temperature whereas basal metabolic rate varies directly, viscous heating could lead to a considerable overestimation of the rate of basal heat production measured micocalorimetrically at low temperatures. Finally, it should be pointed out that, since viscous heating increases with muscle diameter (Fig. 1 *D*), the extent of oxygen diffusion limitation may be underestimated in large muscles at high rates of energy expenditure (Daut and Elzinga, 1988) (see, also, Fig. 3 *B*).

Stimulus heat. To compare the thermal response to hyperosmolality with the maximal rate of active heat production, intact preparations were routinely stimulated briefly at 10 Hz. The magnitude of the stimulus heat was determined by varying both voltage and duration over a range of subliminal stimulation parameters, making use of the fact that stimulus heat varies linearly with stimulus duration but quadratically with stimulus voltage.

Mechanical Measurements

In 11 experiments the effects of elevated osmolality on mechanical performance were examined. The preparations were placed

Published December 1, 1996

in a flow-through organ bath and connected to a force transducer (AE 801, SensoNor, Horton, Norway). Force output was recorded on a 2-channel Gould (2200) chart recorder (Gould Inc., Cleveland, OH); selected twitches were captured on a Gould Oscilloscope Plotter.

Measurement of $[Ca^{2+}]_i$

The ratiometric method of measuring intracellular calcium concentration, $[Ca^{2+}]_i$, which used a modified Zeiss inverted epifluorescence microscope (Carl Zeiss Inc., Thornwood, NY) and commenced with the acetoxymethylester (AM) form of the fluorescent dye Fura-2, has been described in detail previously (van Hardeveld et al., 1995). In brief, trabeculae were isolated and equilibrated in Tyrode solution at 28°C for ~60 min while being stimulated at a frequency of 0.2 Hz. The temperature was then increased to 37°C, and autofluorescence was measured spectrophotometrically at 340 and 380 nm. The preparations were then preincubated at 34°C for 30 min in 10 μmol liter^{-1} Fura-2/AM, dissolved in DMSO, to which had been added 20% (wt/vol) Pluronic F-127 achieving a final concentration of 1%.

In a preliminary series of experiments, the osmolality-dependence of R_{max} (the ratio of fluorescence at 340 nm to that at 380 nm in the presence of saturating levels of Ca^{2+}) and R_{min} (the fluorescence ratio in the absence of Ca^{2+}) were determined (van Hardeveld et al., 1995). R_{max} was followed for 100 min in both isosmotic and hyperosmotic (650 mmol liter^{-1}) Tyrode to which had been added 10 μmol liter^{-1} ionomycin, 2 μmol liter^{-1} CCCP (carbonyl cyanide *m*-chlorophenylhydrazone), 2 mmol liter^{-1} NaCN, and 4 mmol liter^{-1} iodoacetate. R_{min} was followed for 60 min in both isosmotic and hyperosmotic Ca^{2+}-free Tyrode to which had been added 10 mmol liter^{-1} EGTA. R_{max} rose sigmoidally with a half-time of ~30 min, and R_{min} fell exponentially with a half-time of ~20 min. Asymptotic values of R_{max} and R_{min} were 1.03 ± 0.22 (n = 4) and 0.12 (n = 1), respectively. No variation of either parameter with osmolality was apparent.

In selected cases, intracellular Ca^{2+} concentration was estimated from the relationship:

$$[Ca^{2+}]_i = K_d \beta \left(\frac{R - R_{min}}{R_{max} - R} \right), \quad (2)$$

where R is the ratio of the fluorescence emitted in response to excitation at two wavelengths (340 and 380 nm) and β is the ratio of the 380-nm fluorescence signal from Fura-2 in the absence of Ca^{2+} to that recorded in the presence of saturating concentrations (Grynkiewicz et al., 1985). For isosmotic conditions, values of K_d (290 nmol liter^{-1}) and β (3.85) were adopted from an earlier study (van Hardeveld et al., 1995), performed at 20°C, on the assumption that K_d is minimally affected by temperature (Uto et al., 1991). For hyperosmotic conditions, the variation of K_d with ionic strength (I) in vitro is given by: $-\ln K_d = 8.34 - 3.6[2\sqrt{I}/(1 + \sqrt{I}) - 0.4I]$ (Uto et al., 1991). Assuming that the same relationship holds in vivo, then a doubling of ionic strength (subsequent to doubling of osmolality) would be expected to increase the value of K_d by ~30%.

Fluorescence ratios were recorded in six quiescent preparations. After 10 min of isosmotic incubation during which ratios were recorded at 2-min intervals, osmolality was increased to either 450 mosmol l^{-1} (n = 2) or 650 mosmol liter^{-1} (n = 4) by addition of sucrose. In two preparations from the latter group, the hyperosmotic challenge was preceded by 2 min of isosmotic-high-K^+; the preparations were then returned to standard medium for ~30 min before raising the osmolality. In the other two preparations, only the hyperosmotic condition was examined in order to avoid the possibility that pretreatment with isosmotic-high-K^+ may have diminished the subsequent hyperosmotic response.

Statistical Analyses

Nonlinear curve-fitting was performed using the Quasi-Newton method of nonlinear regression available in Systat software (SYSTAT Inc, Evanston, IL). Differences in mean rates of heat production under different conditions, as well as the effect of osmolality on the Fura-2 fluorescence ratio, were examined for statistical significance (at the 95% confidence level) using two-way analysis of variance for repeated measures. Posthoc tests for differences among means were performed using an appropriate set of contrast coefficients. Summary data are presented as mean ± SEM.

RESULTS

Thermal Consequences of Hyperosmolality

The results of a single experiment using a right ventricular trabecula are shown in Fig. 2. 40 min after the calorimeter was closed, by which time thermal equilibration was nearly complete, the rate of heat production of the quiescent preparation under isosmotic conditions was determined by briefly moving it 5 mm downstream (as described in MATERIALS AND METHODS). Under isosmotic conditions, the muscle was then stimulated electrically (*arrows*) for 30 s at 10 Hz using rectangular pulses of 3.5 V. At the first arrow, pulse duration was 300 μs. This was doubled to 600 μs at the second arrow, and the stimulus heat (0.17 μW) was calculated as twice the rate of heat production recorded at the first arrow.

The trabecula was then subjected to a series of hyperosmotic challenges using different chemical species. Between each of these challenges the preparation was returned to isosmotic conditions, and the rate of resting heat production reassessed. The response to 10-Hz stimulation was measured periodically. The stability of both the baseline and the response of the preparation to electrical stimulation over an experiment of some 8 h duration are noteworthy. Upon opening the calorimeter at the end of this period, it was observed that the trabecula still twitched vigorously in response to electrical stimulation.

Characteristics of the thermal response. As is evident in Fig. 2, the increase in rate of heat production in response to an increase of osmolality was very slow compared to the response to electrical stimulation. Having reached a plateau value under hyperosmotic conditions, the rate of heat production could be sustained for many minutes. By contrast, the rate of heat production in response to 10-Hz electrical stimulation, under isosmotic conditions, typically fell during the second half of the 30-s stimulation period (Fig. 2). The response to electrical stimulation during the plateau phase of the hyperosmotic response was negligible under both KCl and NaCl challenge. In sucrose or mannitol the response to electrical stimulation was transiently larger but not sustained. Likewise, it has been reported that raising the osmolality 2.1-fold using mannitol is not fully effective in suppressing the active heat pro-

Published December 1, 1996

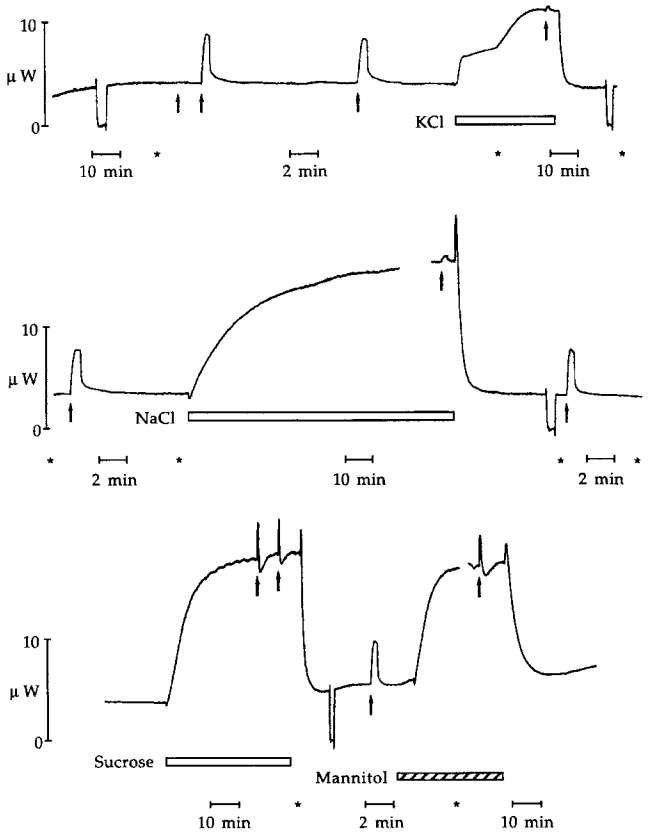

FIGURE 2. Effect of hyperosmolality on resting heat rate. Continuous original record (reproduced by digital scanning) from a slab-shaped trabecula (200 μm × 300 μm × 2.75 mm) of 41.1 μg dry weight. Brief downward deflections reflect movement of preparation 5 mm downstream. Magnitude of downward deflection reflects rate of resting heat production in isosmotic Tyrode. Arrows indicate 30 s of electrical stimulation at 10 Hz (see text); magnitude of upward deflection reflects rate of active heat production. During periods (indicated by *rectangular boxes*) labeled *KCl*, *NaCl*, *Sucrose*, or *Mannitol*, osmolality of standard Tyrode bathing medium increased by 175 mosmol liter^{-1}. Note several changes of time-scale throughout (scale is constant between any pair of stars) but especially during hyperosmotic-high-K^+ treatment. At peak of each hyperosmotic response (*arrows*), muscle stimulated electrically. Occasional discontinuities in trace correspond to change of direction of reciprocating pump that provided flow through measurement chamber.

duction of rabbit papillary muscle (Alpert et al., 1989). The biphasic nature of the thermal response in hyperosmotic-high-K^+ is apparent (*upper trace*, Fig. 2); an initial rapid upstroke, presumably associated with K^+-depolarization (see, also, Fig. 10 *C*), becomes a much slower increase which is associated, in a dose-dependent fashion, with hypertonicity.

An additional feature of the thermal response is exemplified in Fig. 2 (*bottom*). With repeated applications of a hyperosmotic challenge, especially when the dose was high, the rate of heat production under isosmotic conditions became progressively elevated. This behavior seemed to be related to the duration as well as to the magnitude of the hyperosmotic challenge. Provided that the osmotic dose was neither too great nor applied for too great a duration, full recovery of rate of resting heat production to that observed before the hyperosmotic challenge was possible. However, as the osmolality approached ~2.5 times normal, then frequently the isosmotic metabolic rate remained elevated subsequently.

The hyperosmolality–resting heat rate relation. Provided that the data for extremely high osmolalities (where the heat rate fell) were ignored, then the dose-response relation for an individual muscle preparation could be fitted by an analytical expression of the form:

$$\dot{H}(c) = \dot{H}_0 + \dot{H}_1 \frac{c^n}{c_{50}^n + c^n}. \quad (3)$$

In this generalized (four parameter) Hill equation, $\dot{H}$ is the rate of resting heat production as a function of osmolality (or osmotic concentration) c, $\dot{H}_0$ is the asymptotic heat rate at infinite dilution, $(\dot{H}_0 + \dot{H}_1)$ is the asymptotic heat rate at infinite concentration, c_{50} is the osmolality that achieves 50% of the increment from $\dot{H}_0$ to $\dot{H}_1$, and n reflects the "steepness" of the sigmoidal relation. The dose-response relation for a single preparation is shown in Fig. 3 *A*.

From measurements made on 32 preparations (see Table I), the mean (±SEM) measured value of the isosmotic rate of heat production was 100 ± 7 mW (g dry wt)$^{-1}$. The mean (n = 18) hyperosmolality-induced peak rate of heat production was 348 ± 23 mW (g dry wt)$^{-1}$, representing a 3.8 ± 0.25-fold increment with respect to isosmolality. The peak thermal response occurred in the range 450–650 mosmol liter^{-1}, but with considerable variation among preparations, and was uncorrelated with the isosmotic heat rate. Linear regression analyses demonstrated that neither the isosmotic nor peak hyperosmotic rates of heat production depended on muscle thickness. These results are shown in Fig. 3 *B* where heat rates are plotted as a function of cross-sectional area (indexed as dry weight per unit length) and, for ease of comparison with earlier results (Daut and Elzinga, 1988), as equivalent radius (assuming circular cross-sectional area, unit specific gravity, and a wet weight/dry weight ratio of 4.5).

Independence of osmotic species. Although only two experiments specifically addressed the matter, it would appear that the thermal response to hyperosmolality is independent of osmotic species. Comparable results were obtained whether osmolality was increased by NaCl, KCl, mannitol, or sucrose (Figs. 2 and 3 *A*).

Dependence on oxygen. The dependence of the hyperosmotic thermal response on oxygen was examined using three distinct protocols (Fig. 4). Substitution of N_2 for O_2 almost totally abolished the heat production of a trabecula in which the hyperosmotic response had been allowed to develop in the presence of 150 mmol l^{-1} su-

Published December 1, 1996

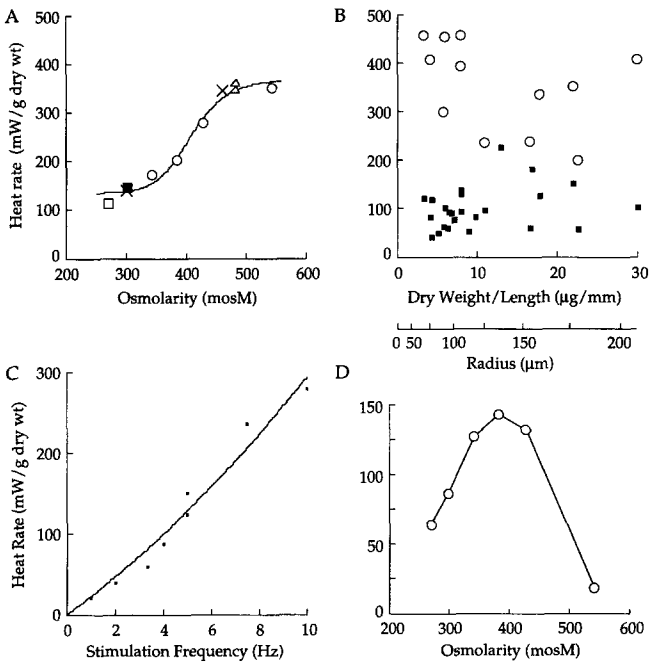

FIGURE 3. Myothermal heat rates. (*A*) Rate of resting heat production as a function of osmolarity and osmotic species for a trabecula of dry weight 38.3 μg and length 1.75 mm. (*filled square*) Isosmolar Tyrode (average of six measurements, SEM smaller than symbol); (*open square*) hypo-osmolarity; (*circles*), added sucrose; (*triangles*) added KCl; (*X*) low Ca^{2+} (80 μmol liter^{-1}): both isosmotic and with added sucrose. Line fitted according to Eq. 3: $\dot{H}_o$ = 145 mW (g dry wt)$^{-1}$, $\dot{H}_1$ = 221 mW (g dry wt)$^{-1}$, c_{50} = 410 mosmol liter^{-1}, n = 15, r^2 = 0.998. (*B*) Isosmotic (*filled squares*) and hyperosmotic (*open circles*) rates of heat production as a function of muscle cross-sectional area indexed as dry weight per unit length (*upper abscissa*) or radius (*lower abscissa*). No significant dependence of either variable on muscle thickness. (*C*) Rate of active heat production ($\dot{H}_a$), under isosmotic conditions, as a function of stimulation frequency (f_s) for a slab-shaped trabecula of width 200 μm, thickness 100 μm, length 2.2 mm, dry weight 14.6 μg, and resting, isosmotic heat rate of 144 mW (g dry wt)$^{-1}$. Equation of quadratic regression line: $\dot{H}_a = 22.1 f_s + 0.72 f_s^2$; r^2 = 0.988. (*D*) Rate of active heat production (in response to 30 s of electrical stimulation at 10 Hz), as a function of osmolality, for a slab-shaped trabecula of width 300 μm, thickness 175 μm, length 1.75 mm, and dry weight 38.3 μg.

crose (Fig. 4 *A*). The reintroduction of oxygen reestablished the hyperosmotic response; return to isosmotic conditions reestablished both the responsiveness of the muscle to electrical stimulation and the isosmotic heat rate (although leaving the latter somewhat elevated). Conversely, doubling of the osmolality in the presence of N_2 failed to elicit the hyperosmotic response (Fig. 4 *B*). After reintroduction of oxygen a very large increase in heat rate was observed, indicating that in the presence of oxygen this muscle could produce a typical hyperosmotic response. Finally, when N_2 and hyperosmolality were simultaneously presented, the depressive effect of the former totally masked the stimulatory effect of the latter (Fig. 4 *C*). These results mirror those of Yamada (1970) who reported a 90% reduction in thermal activity of frog skeletal muscle when N_2 was substituted for O_2 in hypertonic Ringer solution.

TABLE I

Thermal Response to Various Interventions

Condition	n	Basal	Maximal
Hyperosmolality	18	100 ± 7	348 ± 23
10 Hz stimulation	30	99 ± 7	193 ± 18
150 mM KCl	4	99 ± 15	529 ± 60
Ouabain (875 μM)	1	40	730
DNP (91 μM)	5	105 ± 31	710 ± 104

Entries denote mean ± SEM, mW (g dry wt)$^{-1}$, for the number (n) of preparations indicated. Basal and Maximal indicate pretreatment and maximal posttreatment thermal responses, respectively.

Relative magnitude of the thermal response. To assess the relative magnitude of the hyperosmotic thermal response, we compared it to the effects of: (*a*) 10 Hz electrical stimulation, (*b*) isosmotic-high-K^+ (150 mmol liter^{-1} KCl) depolarization, (*c*) a cardiac glycoside, and (*d*) an uncoupler of oxidative phosphorylation.

Each experiment commenced with determination, under isosmotic conditions, of both the rate of resting heat production and the rate of active heat production in response to 30 s of electrical stimulation at 10 Hz (see Fig. 2, for example). In four preparations the active heat-stimulus frequency relation was more fully explored. An example is shown in Fig. 3 *C* where the observed data, corrected for stimulus heat, have been fitted by a quadratic polynomial constrained to pass through the origin. This trabecula, whose dry weight per length was 6.6 μg mm^{-1}, had a resting heat rate of 144 mW (g dry wt)$^{-1}$; under isosmotic-high-K^+ conditions it produced heat at a rate of 370 mW (g dry wt)$^{-1}$.

In Fig. 5 *A* a segment of original record demonstrates a large thermal response to the cardiac glycoside ouabain. Note the comparative rapidity of the response in comparison with that of hyperosmolality which commonly took 20–30 min to stabilize (Fig. 2). The complete ouabain dose-thermal response relation of a single trabecula under isosmotic conditions is shown in Fig. 5 *B*. Note that in this experiment, as in all others of a dose-response nature, the preparation was returned to "control" (in this case, ouabain-free) conditions between measurements.

Brief application of the mitochondrial uncoupling agent dinitrophenol (DNP) also elicited a concentration-dependent thermal response characterized by rapid kinetics (Fig. 5 *C*). Fig. 5 *D* shows the results of two experiments in which the DNP dose-response relation was fully explored and the data fitted according to Eq. 3.

The results of these and other comparative experiments are summarized in Table I. The peak hyperosmotic response was nearly double that of 10 Hz electri-

Published December 1, 1996

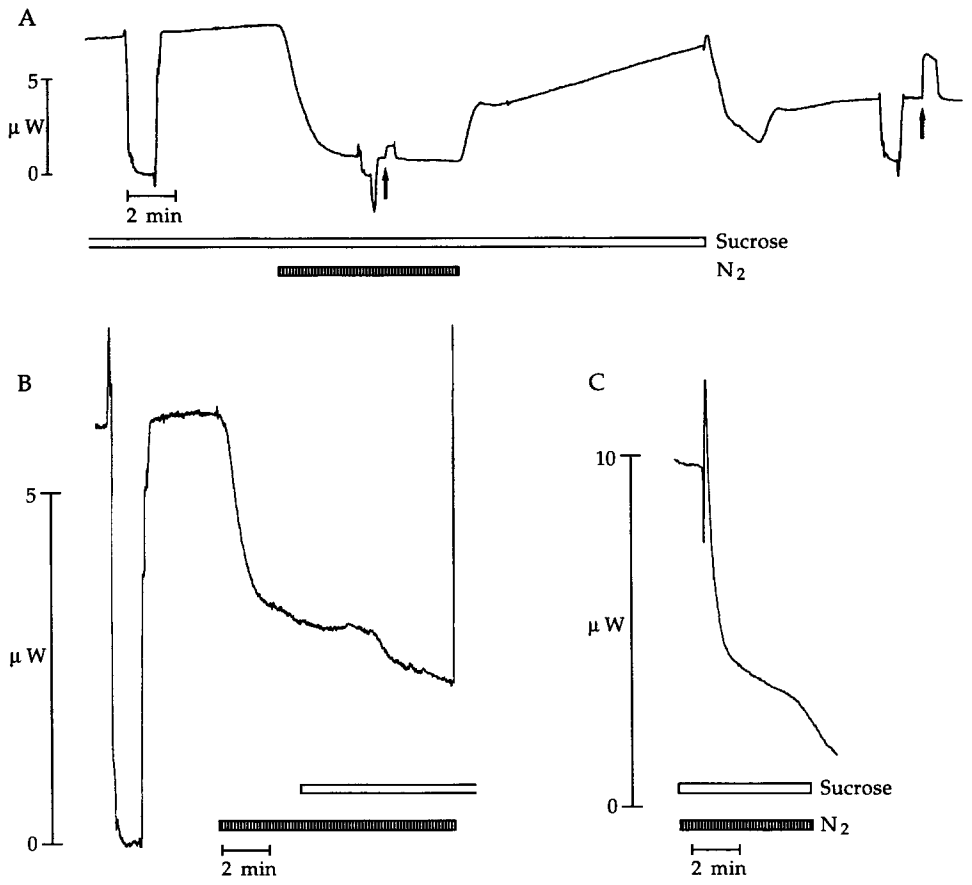

FIGURE 4. Effect of anoxia on hyperosmotic heat rate. (*A*) Original record of rate of heat production of a cylindrical trabecula (diameter 175 μm, length 2.7 mm) of dry weight 21.7 μg. At left-hand side of trace, hyperosmotic response fully developed; rate of heat production 8 μW (four times the previously determined isosmotic rate). N_2 lowered hyperosmotic heat rate to 0.8 μW (large negative deflection during resting heat rate determination in N_2 is a movement artefact). Negligible heat production in response to 10-Hz stimulation (approximately one-half observed response is stimulus heat). Reintroduction of O_2 reestablished the hyperosmotic heat rate. Reintroduction of isosmotic Tyrode (before complete reestablishment of normoxic, hyperosmotic response) lowered rate of heat production, after a complex transient, to 3.4 μW (~70% higher than previously measured under isosmotic conditions). (*B*) Original record of rate of heat production of a slab-shaped trabecula (135 μm × 375 μm × 2.12 mm) of dry weight 38.9 μg. At left-hand side of trace, trabecula had been bathed in standard Tyrode solution for 7.5 h: resting rate of heat production 5.4 μW. N_2 diminished isosmolar heat rate. No effect of increasing osmolality by addition of 300 mmol liter^{-1} sucrose. Reintroduction of O_2 after 6 min: heat rate rose abruptly to 17 μW before declining slowly. (*C*) Same preparation as in *B*; recording commences 14 min later before full recovery of normoxic, isosmotic heat rate (note change of vertical scale). N_2 and 300 mmol liter^{-1} sucrose presented simultaneously without effect.

cal stimulation but was only about two-thirds that of isosmotic-high-K^+ depolarization and one-half of that observed during uncoupling of oxidative phosphorylation (DNP).

In several experiments the rate of active heat production (i.e., in response to electrical stimulation) was determined as a function of osmolality. Active heat rate was potentiated at low to moderate hyperosmolalities but declined abruptly at high osmolarities (Fig. 3 *D*). As shown below, this potentiation of active metabolism occurred despite the inhibition of active force development.

Mechanical Consequences of Hyperosmolality

In a separate set of experiments, isometric force production was measured in a flow-through organ bath. Muscles were paced at a frequency of 2.5 Hz, and the osmolality of the bathing solution varied using sucrose. Two examples are shown in Fig. 6. In Fig. 6 *A* the inhibition of twitch force production by hyperosmolar sucrose at all doses is evident. This is emphasized in *C* by the superimposition of representative steady-state twitches. Note (*A*) the recovery of twitch force upon return to isosmotic conditions and the negligible increase of passive (tonic) force. In Fig. 6 *B*, which shows portions of the results from another experiment, the increase of tonic force under conditions of high osmolality is particularly evident, despite the noisy record.

The mean isometric twitch force-osmolality relation for 11 preparations is shown in normalized form in Fig. 7 *A*. In no case was twitch force enhanced by hyperosmolality. This result, in trabeculae, is consistent with reports of negative inotropy in papillary muscle (Willerson et al., 1978) and whole heart (Ben-Haim et al., 1992*a*, *b*) preparations from the rat. It is in contrast with the behavior of cat papillary muscle in which force is potentiated at osmolalities between 300 and 500 mosmol l^{-1} and is not fully suppressed until osmolality reaches three times normal (Koch-Weser, 1963).

Tonic force development, normalized with respect to peak twitch force, is shown in Fig. 7 *B*; it increased with

Published December 1, 1996

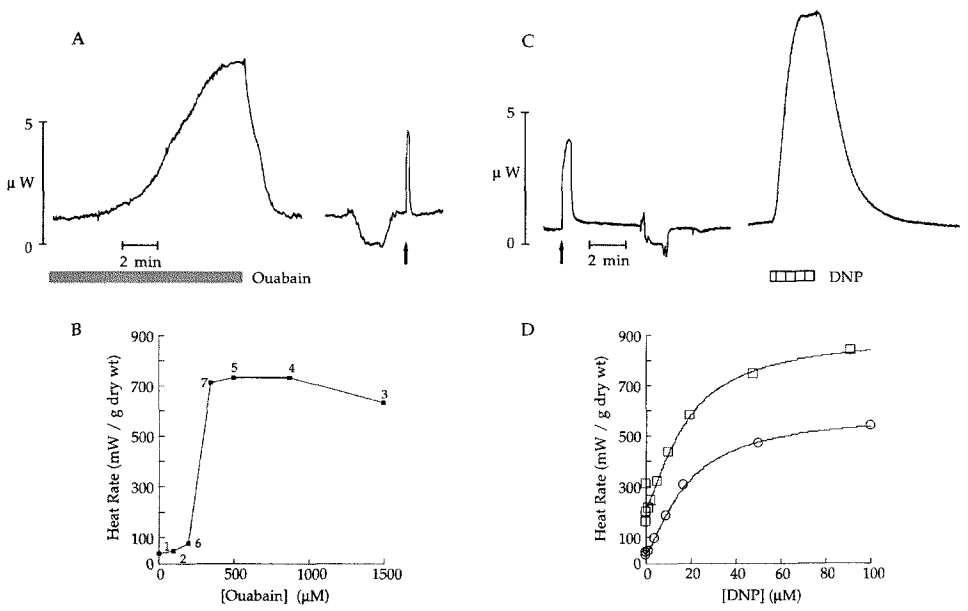

FIGURE 5. Effect of ouabain or DNP on isosmotic heat rates. (*A*) Original record of rate of heat production of a trabecula of dry weight 9.7 μg, diameter 130 μm and length 2.1 mm. Resting heat rate in response to 875 μmol liter^{-1} ouabain (*shaded rectangle*); following the discontinuity: determination of basal and active (in response to 10-Hz electrical stimulation) heat rates in absence of ouabain (stimulus heat 370 nW). (*B*) heat rate as a function of ouabain concentration for same trabecula as shown in *A*; order of presentation of ouabain doses indicated. (*C*) Original record of rate of heat production of a papillary muscle of length 3.1 mm and dry weight 15.9 μg. *Arrow*: 30 s of electrical stimulation (stimulus heat 130 nW); resting heat rate 0.6 μW; following the discontinuity: response to 90.9 μmol l^{-1} DNP. (*D*) Heat rate as a function of DNP concentration. (*circles*) Same muscle as in *C*. (*squares*) Data from a slab-shaped (225 μm × 300 μm × 2.1 mm) trabecula of 27.2 μg dry weight. Solid lines fitted according to Eq. 3: ($\dot{H}_o$, $\dot{H}_1$, c_{50}, n, r^2) = (219, 681, 18, 1.36, 0.9997) and (36, 553, 18, 1.34, 0.9997) for squares and circles, respectively.

osmolality although it rarely exceeded 15% of peak (i.e., isosmotic) active force development.

Inhibition of the Hyperosmotic Thermal Response

We used a number of interventions in an attempt to inhibit the increase in rate of resting heat production in response to hyperosmolality. These were selected on the assumption that the extreme thermal responses shown above reflect the activation of one or more cellular ATPases. The most likely candidates were considered to be the actomyosin ATPase of the cross-bridges, the Na^+-K^+ ATPase of the sarcolemma, and the Ca^{2+} ATPases of the sarcolemmal and sarcoplasmic reticular membranes (Schramm et al., 1994; Ebus and Stienen, 1996).

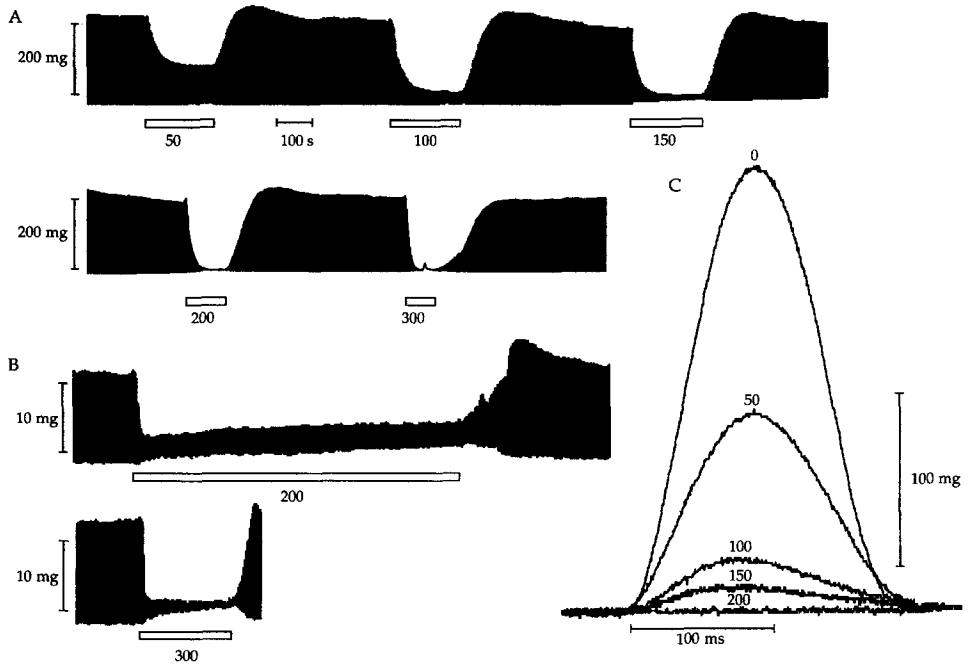

FIGURE 6. Effect of osmolality on force production. (*A*) Right ventricular papillary muscle of circular cross-section (200 μm diameter and 2.72 mm length) and dry weight 24.6 μg. (*B*) Right ventricular trabecula of circular cross-section (100 μm diameter and 2.44 mm length) and dry weight 3.1 μg. Preparations stimulated electrically at 2.5 Hz; slow chart speed fails to distinguish separate twitches. Bathing solution rendered hyperosmotic by addition of sucrose (mmol l^{-1}) for periods indicated by open rectangles. (*C*) Selected steady-state twitches, recorded at higher speed and gain, from *A*.

Published December 1, 1996

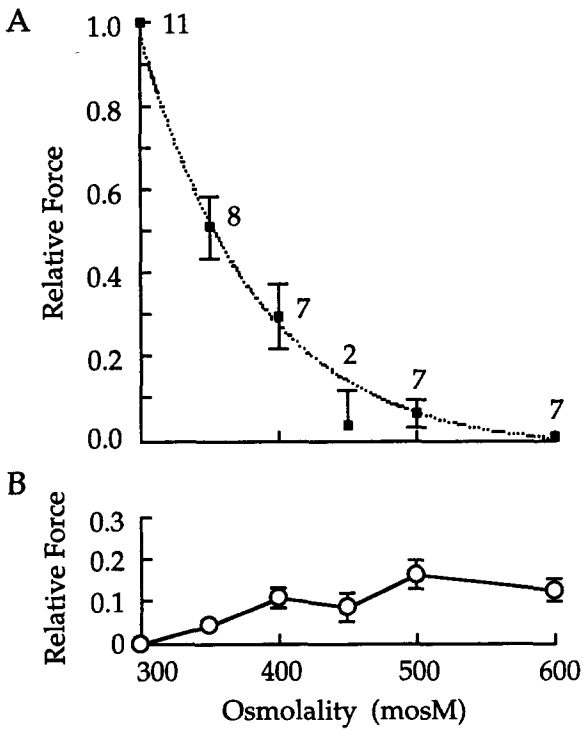

FIGURE 7. Force-osmolality relations. (*A*) Relative active force production (mean ± SEM, number of observations, *n* indicated) in response to 2.5 Hz electrical stimulation. Fitted curve: $y = e^{-0.013x}$; $r^2 = 0.805$. (*B*) Tonic (passive) force development (mean ± SEM, *n* as in *A*) expressed as a fraction of active force development of the same muscle.

Effect of chemical skinning. Given the magnitude of the thermal response to hyperosmolality, it is natural to invoke increased actomyosin ATPase activity as the source. We examined the possibility that hyperosmolality, via mechanical dislocation associated with cell shrinkage, mimics the "trigger" action of Ca^{2+} thereby de-inhibiting the normal suppressive action of tropomyosin on the actin-activated myosin ATPase. We used chemically skinned preparations in which both sarcolemmal and sarcoplasmic reticular membranes are absent. If the usual troponin-tropomyosin inhibition of cross-bridge interaction can be mechanically de-inhibited by cell shrinkage, then we would expect to see an increment of heat production when lateral filament spacing is reduced, even in a bathing medium (the relaxing solution) which is very low in Ca^{2+}.

Three trabeculae were chemically skinned, by incubation in relaxing solution supplemented with 1% Triton X-100, before placement in the calorimeter. The rate of heat production of the relaxed preparation was then determined in the usual way, i.e., by maneuvering it 5 mm downstream using the micromanipulators. An example is shown in Fig. 8 where a skinned trabecula was advanced and returned both in 1-mm steps (*A*) and in single 5-mm steps (*B*). The rate of heat production in relaxing solution was steady over a period of several hours and was uninfluenced by the substitution of N_2 for O_2. Introduction of activating solution caused a repeatable and reversible increase in the rate of heat production, thereby demonstrating the responsiveness of the actomyosin ATPase to Ca^{2+}. But when an increase of osmolality was simulated by addition of PVP to the relaxing solution (*B*), no increment in heat production was observed. In fact, when due account is taken of the dependence of the output of the calorimeter, for a given power input, upon the concentration of PVP (see Fig. 1 *B*), then it is apparent (Fig. 8 *C*) that the rate of heat production of skinned trabeculae diminishes with decreasing interfilament separation (i.e., with increasing PVP concentration).

An estimate of the effectiveness of PVP in effecting lateral compression of the contractile matrix can be derived from results obtained with single skeletal muscle fibers. When an intact frog skeletal fiber is skinned, it experiences an increase in diameter of some 20% (Goldman and Simmons, 1986). Its diameter can be restored to the original value by addition of 4 g dl^{-1} PVP (Matsubara et al., 1984). When a skinned frog fiber is subjected to PVP concentrations comparable to those examined in the current study (5, 10, and 15 g dl^{-1}), it adopts relative diameters of about 0.75, 0.6, and 0.55, respectively (Tsuchiya, 1988). Correcting these values for the above estimate of 20% swelling subsequent to skinning, it may be concluded that skinned trabeculae in the current study adopted diameters of about 0.9, 0.7, and 0.65, respectively, relative to the intact state. To effect comparable extents of compression of intact frog fibers, relative osmolality must be about 1.2, 1.8, and 2.1, respectively (Blinks, 1965). Hence the range of PVP concentration used in the current study should have achieved radial compressions of skinned preparations comparable to those experienced by intact trabeculae under hyperosmotic conditions.

Effect of ouabain. The inhibitory effect of ouabain, a specific inhibitor of the Na^+-K^+ ATPase, upon the rate of resting heat production of guinea-pig trabeculae is brief (Schramm et al., 1994) and is followed by a large, dose-dependent increase (Fig. 5 *B*). The latter phenomenon, which we presume to reflect Na^+_i-dependent stimulation of Ca^{2+} influx via the Na^+-Ca^{2+} exchanger, demonstrates the futility of pretreating trabeculae with ouabain in order to inhibit the hyperosmotic thermal response. Nevertheless, it is possible that any contribution to the thermal response by the Na^+-K^+ pump could be detected by inhibiting the pump. To that end, we introduced 1 mmol $liter^{-1}$ ouabain after a thermal steady state had been reached in 150 mmol $liter^{-1}$ sucrose. In two such experiments (data not shown), ouabain was without effect. These results mimic those of Yamada (1970) who found no effect of ouabain on the

Published December 1, 1996

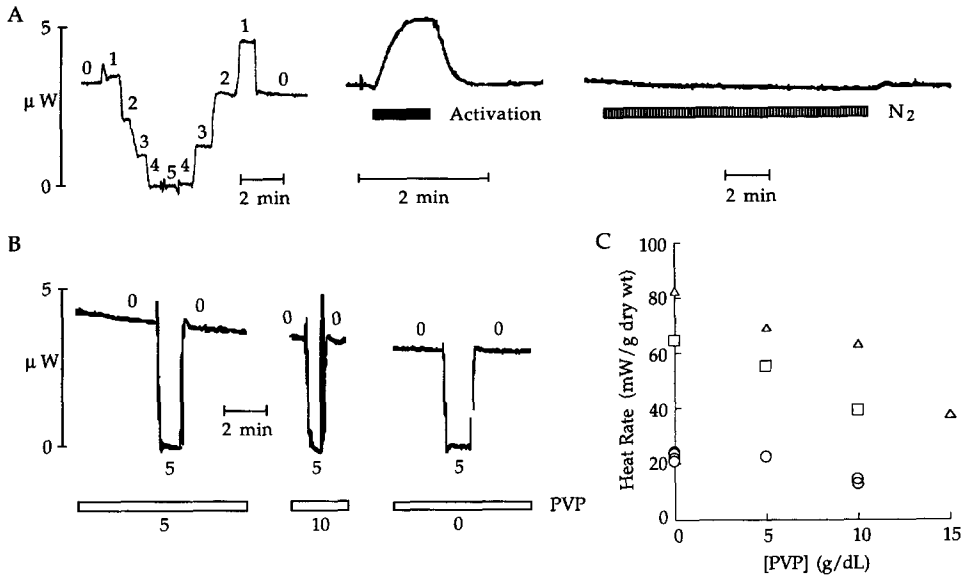

FIGURE 8. Effect of osmolality on rate of heat production of chemically skinned trabeculae. (*A*) Original record from a cylindrical trabecula (diameter 250 μm, length 2.0 mm and dry weight 128.8 μg that had been immersed in skinning solution for 80 min) superfused with relaxing solution and moved (in steps of 1 mm, as indicated) 5 mm downstream out of the measurement chamber and returned; resting heat rate 3 mW g^{-1}. After the first discontinuity: preparation exposed to activating solution for 1 min then to 100% N_2 in relaxing solution for 10 min. (*B*) Same trabecula as in *A*, bathed in relaxing solution containing PVP in concentrations (g dl^{-1}) indicated, moved in single steps of 5 mm downstream out of measurement chamber and returned. Brief discontinuity in rightmost trace: suppression of movement artefact associated with return of trabecula to geometric zero (note presence of artefact in preceding two records). (*C*) Heat rate-[PVP] relations for three chemically skinned preparations bathed in relaxing solution. (*circles*) Data shown in *B*; (*triangles*) trabecula of dry weight 16.5 μg; (*squares*) trabecula of length 2.2 mm and dry weight 13.8 μg; latter two preparations incubated in chemical skinning solution for 30 min.

hyperosmotic response of amphibian skeletal muscle. They are also in accord with the recent finding, using whole-cell patch-clamp techniques, that hyperosmotic shrinkage inhibits Na^+-K^+ pump current in rabbit cardiac myocytes, despite an increase in intracellular Na^+ activity (Whalley et al., 1993).

Effect of extracellular Ca^{2+}. Lowering of $[Ca^{2+}]_o$ from its standard value of 2 mmol $liter^{-1}$ to 125 μmol $liter^{-1}$, 80 μmol $liter^{-1}$ (see Fig. 3 *A*) or 50 μmol $liter^{-1}$ under varying conditions of hyperosmolality, was without effect on the hyperosmotic response. The effect of bathing trabeculae in (nominally) Ca^{2+}-free Tyrode in the face of 150 mmol $liter^{-1}$ sucrose was assessed in four experiments. These results were somewhat more variable. In two experiments the hyperosmotic response was unaffected by Ca^{2+}-free solution; in the third it was increased by 36%, and in the fourth it was decreased by 25%. All four experiments were characterized by poor recovery despite the fact that hyperosmolality inhibits the calcium paradox (Omachi et al., 1994). Nevertheless, from the essentially null results of nine experiments, in which $[Ca^{2+}]_o$ ranged from 0 to 125 μmol $liter^{-1}$, we are confident in concluding that the hyperosmotic stimulation of cardiac resting heat is largely insensitive to the calcium concentration of the bathing medium.

This conclusion was further tested in an experiment in which calcium-free medium was supplemented with 50 μmol $liter^{-1}$ verapamil, an inhibitor of voltage-dependent Ca^{2+} channels. Under isosmotic conditions, verapamil and zero calcium totally suppressed active heat production in response to electrical stimulation. The response to hyperosmotic challenge with 150 mmol $liter^{-1}$ sucrose was undiminished, however, reaching identical values in the presence and absence of verapamil. Comparable null effects of verapamil on the hyperosmotic stimulation of resting, whole-heart oxygen consumption has been recently reported (Hanley et al., 1994*a*). These null effects are consistent with the observation that hyperosmolality hyperpolarizes the cardiac cell membrane (Akiyama and Fozzard, 1975; Lado et al., 1984; Beyer et al., 1986), thereby diminishing Ca^{2+} influx via voltage-dependent Ca^{2+} channels.

Effect of procaine. Since the hyperosmotic response was insensitive to extracellular calcium, we reasoned that it occurs subsequent to elevation of intracellular calcium arising from intracellular sources. Hyperosmolality has been shown to enhance both the rate and extent of binding of ryanodine to the heavy fraction of the sarcoplasmic reticulum (SR) (Ogawa and Harafuji, 1990). Since the binding of ryanodine to the SR places its Ca^{2+}-release channel in an open state (Coronado et al., 1994), it seems plausible that Ca^{2+} release from the SR may be enhanced under hyperosmotic conditions. Hence we examined the effect of procaine, an inhibitor of sarcoplasmic reticular Ca^{2+} release in myocardial tissues (Vornanen, 1987). We used concentrations of either 7 or 11 mmol $liter^{-1}$. These doses were chosen both because they diminish the hyperosmotic response in skeletal muscle (Yamada, 1970) and because, under isosmotic conditions, they completely inhibit active force production of rat trabeculae in response to elec-

Published December 1, 1996

trical stimulation (I. Erac and D.S. Loiselle, unpublished observations).

The results are shown in Fig. 9 *A* where the ability of procaine to suppress the hyperosmotic thermal response is seen to depend inversely on the cross-sectional area of the preparation. In sufficiently small trabeculae, in which penetration was presumably not diffusion limited, procaine fully suppressed the hyperosmotic response. An example is shown in Fig. 9 *B* where 11 mmol liter^{-1} procaine repeatably abolished the hyperosmotic response to 150 mmol liter^{-1} sucrose. The small size of this preparation precluded detection of its resting heat production.

A secondary effect of procaine is displayed in Fig. 9 *C*. In preparations that were sufficiently large to make accurate measurements, the isosmotic rate of resting heat production was moderately and reversibly potentiated by procaine. A similar effect of procaine on the rate of oxygen consumption of the isolated, guinea-pig heart has been recently reported (Hanley et al., 1994*a*) as has that of the closely allied agent tetracaine on the isosmotic heat rate of resting rat skeletal muscle (Chinet and Giovannini, 1989).

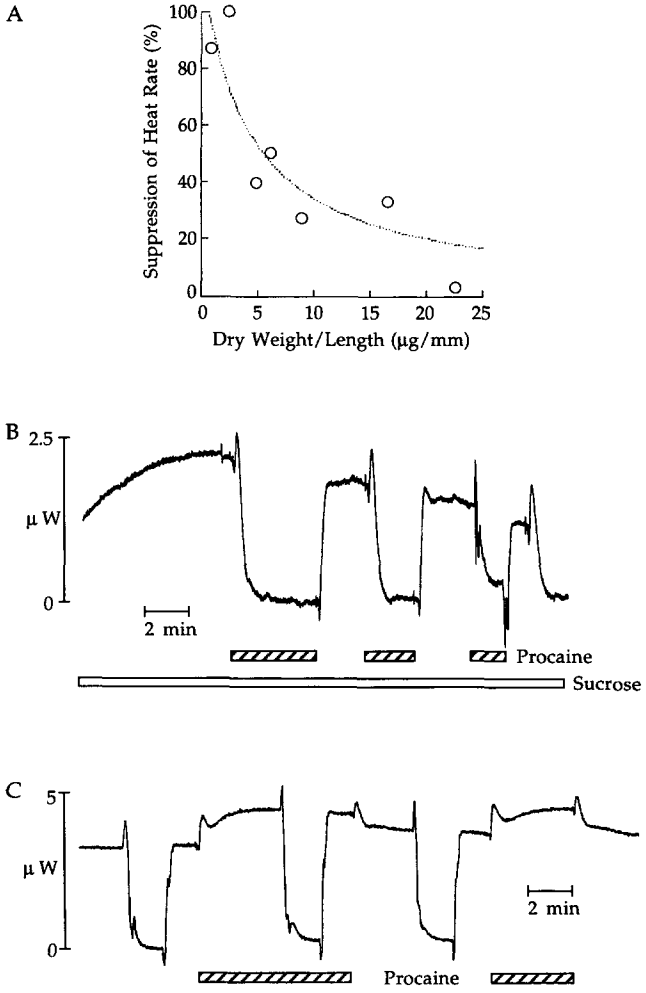

FIGURE 9. Effect of procaine on rates of resting heat production. (*A*) Relative suppression (%) of hyperosmotic heat rate by procaine (7 or 11 mmol l^{-1}) as a function of cross-sectional area (dry weight/length) of 7 trabeculae. Line fitted by hyperbolic relation: $y = 985/(x + 7.48) - 23.2$; $r^2 = 0.945$. (*B*) Original record of rate of heat production of a cylindrical trabecula (diameter 95 μm, length 1.72 mm, dry weight 4.3 μg) bathed in 150 mmol liter^{-1} sucrose. Procaine (11 mmol liter^{-1}), periodically applied, abolished hyperosmotic response. Muscle too small to detect isosmotic rate of resting heat production. (*C*) Original record from a cylindrical trabecula (diameter 225 μm, length 2.25 mm, dry weight 50.8 μg). Procaine (7 mmol liter^{-1}) reversibly increased resting heat rate about 25% under isosmotic conditions.

Effect of Hyperosmolality on $[Ca^{2+}]_i$

Increasing osmolality from its standard value of 300 mosmol liter^{-1} to either 450 mosmol liter^{-1} or 650 mosmol liter^{-1} had only a modest effect on *R*, the Fura-2 fluorescence ratio (Fig. 10 *A*). When averaged across both osmotic conditions, the mean value observed between 2 and 15 min, 0.242 ± 0.0076 (n = 42), was significantly greater than the mean value recorded, at t = 0, under isosmotic conditions: 0.222 ± 0.012 (n = 6). If we accept the limitations of the current calibration procedure, then this 10% increment in R would represent a 20% increase of $[Ca^{2+}]_i$ from ~140 to ~170 nmol liter^{-1} or from a pCa of ~6.85 to ~6.75. If we correct for the variation of K_d with ionic strength (see MATERIALS AND METHODS: *Measurement of* $[Ca^{2+}]_i$), then the increase of $[Ca^{2+}]_i$ could be as large as 30%.

In contrast to the minimal response in hyperosmotic sucrose solution, isosmotic-high-K^+ increased R from 0.19 ± 0.05 to 0.51 ± 0.30, corresponding to a rise from ~100 to ~840 nmol liter^{-1}. This increment occurred within 30 s (Fig. 10 *B*), a time interval that is consistent with both the thermal (Fig. 10 *C*) and mechanical (Fig. 10 *D*) responses to isosmotic-high-K^+. The contrast between the responses to isosmotic-high-K^+ and to hyperosmolality is profound. In a quiescent trabecula, isosmotic-high-K^+ causes a transient increase of $[Ca^{2+}]_i$ (Fig. 10 *B*), a transient increase of heat rate (Fig. 10 *C*) and a transient contracture (Fig. 10 *D*). Hyperosmotic-high-K^+ has no effect on tonic tension (Fig. 10 *D*), causes a biphasic increase of heat rate (Fig. 2), and, by analogy with the negligible effect of hyperosmolality shown in Fig. 10 *A*, would be expected to have little effect on $[Ca^{2+}]_i$.

DISCUSSION

When the osmolality of the solution bathing quiescent trabeculae from the right ventricle of the rat is increased, the rate of heat production undergoes a slow increase that depends on the dose but not on the osmotic species (Figs. 2 and 3 *A*). The hyperosmotic thermal response is absolutely dependent on oxygen (Fig. 4). It is accompanied by a diminution of active force

Published December 1, 1996

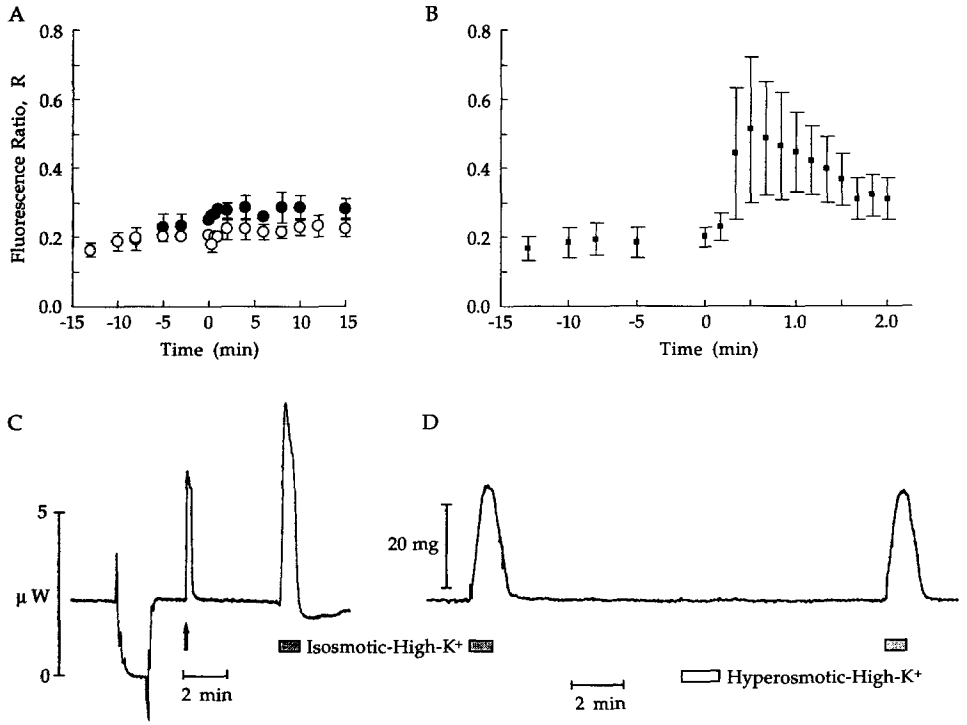

FIGURE 10. Contrasting effects of hyperosmolality and isosmotic-high-K^+ on heat, force and $[Ca^{2+}]_i$. (*A*) Fura-2 fluorescence ratio, *R* (see Eq. 2, text) as a function of time, for trabeculae incubated in either 450 mosmol $liter^{-1}$ (*filled circles*, $n = 2$) or 650 mosmol l^{-1} (*open circles*, $n = 4$) achieved by addition of sucrose. (*B*) *R* as a function of time for trabeculae incubated in isosmotic-high-K^+ ($n = 2$). (*C*) Resting heat rate followed by active heat rates in response to 10-Hz electrical stimulation (*arrow*) and isosmotic-high-K^+ (*shaded rectangle*) of a trabecula of length 1.75 mm, dry weight 13.9 μg, and elliptical cross-section. (*D*) Force as a function of time for a trabecula (same one as in Fig. 6 *B*) exposed to isosmotic-high-K^+ before and after exposure to hyperosmotic-high-K^+ achieved by addition of 150 mmol $liter^{-1}$ KCl to standard Tyrode solution (*open rectangle*).

production (Figs. 6 and 7 *A*) together with small increments of passive (tonic) force (Figs. 6 and 7 *B*) and intracellular calcium concentration, $[Ca^{2+}]_i$, (Fig. 10 *A*). The magnitude of the peak steady-state thermal response to hyperosmolality is considerable. It exceeds the maximal rate of active heat production in response to 10-Hz electrical stimulation under isosmotic conditions and is about one-half as large as that measured when oxidative phosphorylation is uncoupled (Table I).

The unimportance of osmotic species in generating the metabolic response seems to be a general phenomenon. Various combinations of NaCl, sucrose, mannitol, and sorbitol have been found equally capable of stimulating CO_2 production in rat hemidiaphragm (Kuzuya et al., 1965) and heat production of frog skeletal muscle (Yamada, 1970), as well as uptake and metabolism of glucose in rat adipose tissue and skeletal muscle (Clausen, 1968; Clausen et al., 1970). In isolated, KCl-arrested, guinea-pig hearts, 350 mmol $liter^{-1}$ mannitol and sucrose have been found to have comparable potentiating effects on the rate of oxygen consumption (Hanley et al., 1994*a*). Such independence of osmotic species (see, also, Figs. 2 and 3 *A*) gives confidence that the observed metabolic effects reflect diminution of cell volume per se with its attendant increase of intracellular ion concentrations and, hence, ionic strength and osmolality.

Energy Expenditure

Comparison with skeletal muscle. Yamada (1970) reported a 10- to 20-fold increase in the rate of heat production of frog sartorii resting on a thermopile at 20°C when the osmolality was increased 2.5- to 3-fold. This is much larger than the roughly fourfold increase observed in the current study and may reflect the fact that the resting metabolism of cardiac muscle accounts for a much greater fraction of the total than in skeletal muscle (Loiselle, 1987). But the absolute values reported by Yamada, 20–50 mcal $(g\ wet\ wt)^{-1}\ min^{-1}$, corresponding to about 10 mW $(g\ dry\ wt)^{-1}$, are only about one-fortieth of the peak steady-state values that we observed. This difference in absolute rates cannot likely be accounted for by the 17°C difference in temperature but may reflect the much lower mitochondrial volume fraction and, hence, oxidative capacity of skeletal muscle compared with that of cardiac muscle (Loiselle, 1987). In support of this contention, Chinet and Giovannini (1989) found that doubling the osmolality of the solution incubating rat soleus muscles at 30°C produced a rate of heat production corresponding to about 40 mW $(g\ dry\ wt)^{-1}$, i.e., about one-tenth of that observed in rat ventricular trabeculae at 37°C in the current study. In the isolated, perfused rat heart, doubling of the osmolality causes a fivefold increase in the rate of resting oxygen consumption to ~45 μmol min^{-1} $(g\ dry\ wt)^{-1}$ (Hanley et al., 1994*a*). Assuming an energetic equivalent of 450 kJ $(mol\ O_2)^{-1}$ (Chinet and Giovannini, 1989), this corresponds to about 330 mW $(g\ dry\ wt)^{-1}$, a value in close accord with the mean of 348 mW $(g\ dry\ wt)^{-1}$ found in the current study (Table I).

Comparison with metabolic uncoupling. The rate of heat production under hyperosmotic conditions was only about 50% of that evoked by DNP under isosmotic con-

Published December 1, 1996

ditions (Table I) while its time-course of potentiation was much slower (contrast Figs. 2 and 5 *C*). Nevertheless, both the magnitude of the hyperosmotic thermal response and its critical dependence on oxygen (Fig. 4) are consistent with the possibility that hyperosmolality uncouples oxidative phosphorylation by short-circuiting the flow of protons through the F_0-F_1 ATP synthase. Studies of isolated mitochondria, however, convincingly demonstrate that hyperosmolality inhibits oxidative phosphorylation (Slater and Cleland, 1953; Nicholls et al., 1972), probably by inhibition of adenine nucleotide translocase (Chávez et al., 1987). In fact, under isosmotic conditions, increased rates of oxidative phosphorylation are associated with an increase of mitochondrial volume (Halestrap, 1989) whereas mitochondria shrink in hypertonic media (Sperelakis and Rubio, 1971). Hence, any increase of osmolality, without concurrent increase of energy demand, would be expected to inhibit oxidative phosphorylation. It thus seems unlikely that the increased rate of heat production observed in the current study can be attributed to uncoupling of mitochondrial oxidative phosphorylation. We favor, instead, the interpretation that hyperosmolality increases cellular energy demand and, hence, oxidative phosphorylation, an interpretation consistent with the critical dependence of the hyperosmotic thermal response on the presence of oxygen (Fig. 4).

Energy Demand

Under isosmotic conditions, cardiac energy demand increases in response to increasing intracellular Ca^{2+} concentration (Fiolet et al., 1995). Under hyperosmotic conditions, the peak thermal response in the current study occurred in the range 450–650 mmol liter^{-1}. At either osmolality, only a modest increase of $[Ca^{2+}]_i$ was observed (Fig. 10 *A*). This result contrasts with that of Lado et al. (1984) who showed, using Ca^{2+}-sensitive microelectrodes, a fourfold increase of resting Ca^{2+} activity (to ~400 nmol liter^{-1} or pCa of 6.4) in ovine ventricular tissue when tonicity was doubled. It is of interest that these authors found considerable tonic tension to be developed under hypertonic conditions and that they consider the $[Ca^{2+}]_i$ "threshold" for the development of tonic tension to be ~200 nmol l^{-1}. In rat trabeculae, $[Ca^{2+}]_i$ did not exceed this putative threshold (Fig. 10 *A*) nor was there a dramatic increase of resting tension (Figs. 6 and 7 *B*). There was, however, a small increase of $[Ca^{2+}]_i$. What could be its source?

Source of Ca^{2+}. We consider it unlikely that the source of Ca^{2+} is extracellular. Varying $[Ca^{2+}]_o$ under hyperosmotic conditions has minimal effects on either heat production (see RESULTS) or myocardial oxygen consumption (Hanley et al., 1994*a*). Similar null results accompany inhibition of voltage-dependent Ca^{2+} channels using either verapamil (Kent et al., 1983; Hanley et al., 1994*a*) (and see RESULTS) or D600 (Willerson et al., 1978).

Evidence from both the current study and previous studies implicates the sarcoplasmic reticulum as the source of Ca^{2+}. Fig. 3 *D* shows enhancement of active heat production over a range of osmolalities in which active force production is inhibited (cf., Fig. 7 *A*). One explanation for this behavior is that hyperosmolality causes a decrease of force-dependent heat which is compensated by an even larger increase of force-independent heat. The latter component is widely interpreted as the thermal accompaniment of Ca^{2+} uptake by the SR (Alpert et al., 1989). In support of this interpretation, Ca^{2+} transients in ferret papillary muscle are enhanced under hyperosmotic conditions, even at osmolalities where active force production is diminished (Allen and Smith, 1987). Hence it is unlikely that the Ca^{2+} content of the SR is depleted by hyperosmolality. This conclusion has been independently inferred from measurement of the force production of mechanically skinned, single skeletal muscle fibers (Lamb et al., 1993) as well as from observations of osmolality-dependent intracellular acidosis (Whalley et al., 1994). These various thermal, ionic, and mechanical data suggest an increase in the amount of Ca^{2+} that can be released from the SR under hyperosmotic conditions. Since an increase of ionic strength is capable of releasing Ca^{2+} from isolated SR microsomes (Martonosi and Feretos, 1964), the modus operandi for Ca^{2+} release under hyperosmotic conditions may be indirect, via shrinkage-induced increase in ionic strength of the cytoplasm.

Further evidence that the source of Ca^{2+} is sarcoplasmic reticular is provided in Fig. 9 where the local anesthetic procaine is seen to be capable of inhibiting the hyperosmotic thermal response (fully, in sufficiently small preparations). In preparations ranging from isolated SR vesicles through disaggregated myocytes and cell bundles to the perfused whole heart, procaine has been shown to antagonize both caffeine- and Ca^{2+}-induced release of Ca^{2+} from the SR (see Hanley et al., 1994*a*, and references therein). The ability of procaine to inhibit the thermal response to hyperosmolality in cardiac trabeculae (Fig. 9) accords with other studies in which either procaine or tetracaine have been shown to diminish hyperosmolality-induced increments of tonic force (Lännergren and Noth, 1973; Clausen et al., 1979), oxygen consumption (Hanley et al., 1994*a*), and heat production (Yamada, 1970; Chinet and Giovannini, 1989) under hyperosmotic conditions. Dantrolene, another inhibitor of SR Ca^{2+} release, also suppresses the energetic responses of muscle to hypertonicity (Chinet and Giovannini, 1989), thereby lending further support to the contention that the source of increased $[Ca^{2+}]_i$ under hyperosmotic conditions is sarcoplasmic reticular.

Published December 1, 1996

Thermal Sources

Given a (modest) increase of $[Ca^{2+}]_i$ during hyperosmotic challenge, four possible thermal sources require consideration: cross-bridge actomyosin ATPase, sarcolemmal Na^+-K^+ ATPase, the Ca^{2+} ATPases of the sarcolemmal and sarcoplasmic reticular membranes, and the ATP synthase of the inner mitochondrial membrane.

Actomyosin ATPase. It might be expected that any increase of intracellular Ca^{2+} activity associated with hyperosmolality would increase active force development under hyperosmotic conditions. However, the contrary occurs. Maximal Ca^{2+}-activated force development of skinned fibers decreases when interfilament lateral spacing is reduced by use of high molecular weight dextrans or PVP. This result obtains in both skeletal (Goldman and Simmons, 1986; Tsuchiya, 1988) and cardiac (de Beer et al., 1988) preparations and probably reflects the inhibitory effect on force production of: (*a*) increased ionic strength (Kentish, 1984; Kawai et al., 1990), (*b*) lateral compression of the contractile matrix (Fortune et al., 1994), and (*c*) decreased Ca^{2+} sensitivity of the contractile proteins which accompanies both hyperosmolality (Lamb et al., 1993) and elevated ionic strength (Kentish, 1984). The loss of Ca^{2+}-sensitivity is such as to render the aforementioned intracellular pCa values of 6.8–6.4 essentially ineffective in activating actomyosin ATPase.

Hence the diminution of active force production seen in intact preparations under either hyperbaric (Fortune et al., 1994) or hyperosmotic (Fig. 7 *A*) conditions can be attributed to compressive effects on the contractile proteins per se. Whereas cross-bridges probably form, since there is an increase of both tonic force (Fig. 7 *B*) and stiffness (Allen and Smith, 1987; Månsson, 1994), their kinetics may be slowed since velocity of contraction is much reduced (Edman and Hwang, 1977; Gulati and Babu, 1984; Metzger and Moss, 1987; Ford et al., 1991). Moreover, the actomyosin ATPase activity of chemically skinned preparations is inhibited by osmotic compression in either the presence (Krasner and Maughan, 1984; Zhao and Kawai, 1993) or absence (Fig. 8) of Ca^{2+}, as well as by an increase of ionic strength (Kawai et al., 1990), an obligatory consequence of increased osmolality. The question thus arises: could the observed passive force (~15% of isosmotic twitch force [Fig. 7]) reflect significant actomyosin ATPase activity? The linear dependence of heat production on stress-time integral during active contractions (Loiselle, 1987; Schramm et al., 1994) allows this question to be addressed quantitatively.

We determined the force-time integral of a single, steady-state twitch developed by a trabecula in response to 2-Hz electrical stimulation. We then compared this value with the one that would have arisen over the same 500-ms interval if 15% of peak twitch force had been developed tonically (i.e., in the absence of electrical stimulation). The force-time integral of the single twitch was 33.9 μN s. The peak force reached during the twitch was 0.685 μN. Hence the force-time integral expected under hyperosmotic conditions (i.e., if 15% of peak twitch force had been developed) would have been 51.4 μN s (0.15 × 685 μN × 0.5 s), a value some 50% greater than that of a single twitch. Thus a 50% greater rate of heat production might be expected under hyperosmotic conditions, when twitch force is abolished but tonic force is increased, than during a train of steady-state twitches at 2 Hz. However, the rate of active heat production during twitch contractions at a stimulation frequency of 2 Hz is only about 15% of that developed at 10 Hz (Fig. 3 *C*). The heat rate at 10 Hz, in turn, is little more than one-half of that observed during hyperosmotic challenge (Table I). So, even if no correction is made for the slowing in rate of cross-bridge cycling that is presumed to accompany hyperosmolality (see above), heat production arising from actomyosin ATPase activity is unlikely to account for more than 10–15% of the thermal response observed under hyperosmotic conditions. Contrariwise, if a 50% increase of passive force-time integral is solely responsible for a 12-fold increase of heat production, the rate of cross-bridge cycling would have to increase about 8-fold.

Na^+-K^+ ATPase. Hyperosmolality causes an increase of $[Na^+]_i$ (Lado et al., 1984; Whalley et al., 1993). This is attributable to cell shrinkage per se as well as to $Ca^{2+}{}_i$-dependent Na^+-influx via the sarcolemmal Na^+-Ca^{2+} exchange mechanism. Increase of $[Na^+]_i$ would be expected to stimulate activity of the sarcolemmal Na^+-K^+ ATPase. But hyperosmolality inhibits the Na^+-K^+ pump by decreasing its affinity for $Na^+{}_i$ (Whalley et al., 1993). Since the Na^+-pump contributes less than 10% to cardiac resting metabolism under isosmotic conditions (Schramm et al., 1994), we infer that its inhibition by hypertonicity must render its contribution negligible. Indeed, we observed no detectable change of heat rate when 1 mmol liter^{-1} ouabain was introduced after a hyperosmotic thermal steady state had been achieved (see RESULTS).

Mitochondrial Ca^{2+} transport. Any increase of cytoplasmic Ca^{2+} concentration during hyperosmotic challenge would also be expected to increase intramitochondrial Ca^{2+} activity (Miyata et al., 1991). But, as one of us has argued elsewhere (Hanley et al., 1994*b*), the metabolic cost of extruding mitochondrial Ca^{2+} is negligible, under isosmotic conditions. Given that hyperosmolality acts to diminish the oxidative capacity of isolated mitochondria (see above), it seems unlikely that hyperosmolality-enhanced mitochondrial Ca^{2+} transport could represent a significant thermal source under hyperosmotic conditions. It could, however, underlie the slow progressive increase of isosmotic heat pro-

duction observed in rat trabeculae following repeated hyperosmotic challenges (Fig. 2).

Ca^{2+} ATPases. It has been posited above that hyperosmolality increases the efflux of Ca^{2+} from the SR. We now propose that the resulting modest increment of $[Ca^{2+}]_i$ (Fig. 10 *A*) is the consequence of greatly increased Ca^{2+} ATPase activity in the face of this enhanced efflux. This is unlikely to be due in any great measure to the sarcolemmal Ca^{2+} pump. Whereas it has a high affinity for Ca^{2+}, its capacity is low and probably saturated under isosmotic conditions (Carafoli, 1985; Ponce-Hornos, 1989). Hence its contribution to the hyperosmotic thermal effect can probably be ignored. This conclusion is bolstered by the observation that reducing $[Ca^{2+}]_o$, a condition that would favor Ca^{2+} extrusion via the sarcolemmal pump, had no effect on the hyperosmotic thermal response (see RESULTS).

The SR Ca^{2+} pump, by contrast, accounts for a greater proportion of active metabolism under isosmotic conditions: estimates include 15% of heat production (Schramm et al., 1994), 18% of ATPase activity (Ebus and Stienen, 1996), and 30% of oxygen consumption (Loiselle, 1987). Hence increased efflux of Ca^{2+} from the SR could allow its Ca^{2+} pumps to make a substantial contribution to the hyperosmotic thermal response. Such a contribution would constitute a "futile cycle" in the sense that energy is expended to pump Ca^{2+} from the cytoplasm back into an intracellular compartment that has been rendered leaky by the prevailing hyperosmotic environment. The contribution is "non-futile" in the sense that elevated activity of the pump keeps $[Ca^{2+}]_i$ relatively low. The ability of procaine, a drug that inhibits SR Ca^{2+} efflux (Vornanen, 1987), to blunt the thermal (Fig. 9) and oxidative (Hanley et al., 1994*a*) responses to hyperosmolality in rat cardiac tissue further supports the suggestion of a substantial energetic contribution by the Ca^{2+} ATPase of the sarcoplasmic reticulum.

The sustained nature of the thermal response to hyperosmolality demands that, in addition to futile cycling of Ca^{2+} by the SR, Ca^{2+} extrusion across the sarcolemma must also be inhibited. Evidence in support of this contention has recently been reported. From a study of the mechanical behavior of isolated rat trabeculae, it was inferred that the net forward rate of the sarcolemmal Na^+-Ca^{2+} exchanger is diminished under hyperosmotic conditions (Erac et al., 1996).

Conclusion. Increasing the osmolality of the solution bathing an isolated, quiescent, cardiac trabecula causes a large increase in its rate of heat production. The increase occurs despite the inhibition of active force development and is associated with only modest increments of both passive (tonic) force development and intracellular Ca^{2+} activity. Procaine, an agent that is known to inhibit Ca^{2+} release from the SR, is capable of fully inhibiting the thermal response, at least in preparations of sufficiently small diameter. One possible interpretation of these observations is that hyperosmolality simultaneously causes release of Ca^{2+} from the sarcoplasmic reticulum while inhibiting sarcolemmal Na^+-Ca^{2+} exchange. The resultant increase of cytoplasmic Ca^{2+} concentration stimulates the SR Ca^{2+}-ATPase. Enhanced pump activity, in turn, maintains the observed low concentration of intracellular Ca^{2+}. It seems unlikely that increased activity of the SR Ca^{2+}-ATPase can account for all of the heat that is observed under hyperosmotic conditions. The remainder probably reflects an increased extent of Ca^{2+}-activated actomyosin ATPase activity, commensurate with the aforementioned modest increment of resting force production, despite the fact that hyperosmotic shrinkage inhibits the rate of ATP hydrolysis by cross-bridges.

APPENDIX

Viscous heating reflects conversion into heat of the mechanical work of deformation of a moving fluid. In the particular case modeled in Fig. 1 *C*, the fluid is typically physiological saline, and impediment to its flow arises from the presence of a trabecula that is positioned coaxially within a tube of radius b. For the purpose of simplification, the trabecula is modeled as a circular cylinder of radius a and length L. Fluid, of viscosity η, flows past it at a constant volumetric rate $\dot{V}$.

The velocity field for this simple annular flow is well known (Bird et al., 1960). The steady-state velocity is axial (as indicated in Fig. 1 *C*) and its magnitude ω varies with radial distance, r, according to:

$$\omega(r) = \frac{\Gamma}{4\eta}\left[r^2 - a^2 - (b^2 - a^2)\frac{\ln(r/a)}{\ln(b/a)}\right], \qquad (A1)$$

where Γ is the pressure gradient in the axial direction. The model ignores end effects, an assumption that is well met when $(b - a)/L$ is small.

The rate of viscous heating per unit volume, $\dot{H}_v$, is given in terms of the fluid velocity gradient by the so-called "dissipation function" which, in this simple case, reduces to $\eta(d\omega/dr)^2$ (Bird et al., 1960). Inserting ω from Eq. A1 into this expression, the rate of viscous heating per unit length is given by:

$$\frac{\dot{H}_v}{L} = 2\pi\int_a^b \eta\left[\frac{d\omega}{dr}\right]^2 r\,dr = \frac{\pi\Gamma^2 b^4}{8\eta}(1 - \zeta^{-4}), \qquad (A2)$$

where $\zeta = (b/a)$. The volumetric flow rate is given by:

$$\dot{V} = 2\pi\int_a^b \omega(r)\,r\,dr = \frac{\pi\Gamma b^4}{8\eta}(1 - \zeta^{-2})\left[\frac{1 - \zeta^{-2}}{\ln\zeta} - (\zeta^{-2} + 1)\right]. \qquad (A3)$$

Elimination of the pressure gradient, Γ, between Eqs. A2 and A3, and defining the dimensionless geometric factor:

$$\Psi(\zeta) = \frac{\zeta^4}{\zeta^4 - 1}\left[1 - \frac{\zeta^2 - 1}{\zeta^2 + 1}(\ln^{-1}\zeta)\right]^{-2}, \qquad \text{(A4)}$$

yields the required expression for the rate of viscous heating as a function of volumetric flow rate, $\dot{V}$:

$$\frac{\dot{H}_v}{L} = \frac{8\mu}{\pi b^4}\Psi(\zeta)\,\dot{V}^2. \qquad \text{(A5)}$$

The generous support of the Netherlands NWO is gratefully acknowledged by D. Loiselle. We express our appreciation for the unfailing technical assistance provided throughout the course of this study by Ronald Buitenweg, Foppo Dijkema, Peter Sneekes, and Ko van der Lubbe. It is a pleasure to thank Fiona Cameron for scanning of the original records and Patricia Cooper for preparation of the Figures.

Original version received 4 March 1996 and accepted version received 16 September 1996.

REFERENCES

Akiyama, T., and H.A. Fozzard. 1975. Influence of potassium ions and osmolality on the resting membrane potential of rabbit ventricular papillary muscle with estimation of the activity and the activity coefficient of internal potassium. *Circ. Res.* 37:621–629.

Allen, D.G., and G.L. Smith. 1987. The effects of hypertonicity on tension and intracellular calcium concentration in ferret ventricular muscle. *J. Physiol. (Lond.).* 383:425–439.

Alpert, N.R., E.M. Blanchard, and L.A. Mulieri. 1989. Tension-independent heat in rabbit papillary muscle. *J. Physiol. (Lond.).* 414: 433–453.

Ben-Haim, S.A., Y. Edoute, G. Hayam, and O.S. Better. 1992*a*. Sodium modulates inotropic response to hyperosmolarity in isolated working rat heart. *Am. J. Physiol.* 263:H1154–H1160.

Ben-Haim, S.A., G. Hayam, Y. Edoute, and O.S. Better. 1992*b*. Effect of hypertonicity on contractility of isolated working rat left ventricle. *Cardiovasc. Res.* 26:379–382.

Beyer, T., L.S. Jepsen, H. Lüllmann, and U. Ravens. 1986. Responses to hypertonic solutions in guinea-pig atria: changes in action potentials, force of contraction and calcium content. *J. Mol. Cell. Cardiol.* 18:81–89.

Bird, R.B., W.E. Stewart, and E.N. Lightfoot. 1960. Transport Phenomena. John Wiley and Sons, New York. 780 pp.

Blinks, J.R. 1965. Influence of osmotic strength on cross-section and volume of isolated single muscle fibres. *J. Physiol. (Lond.).* 177:42–57.

Carafoli, E. 1985. The homeostasis of calcium in heart cells. *J. Mol. Cell. Cardiol.* 17:203–212.

Chapman, R.A. 1978. The effects of changes of the tonicity of the bathing fluid upon the tension generated by atrial trabeculae isolated from the heart of the frog, *Rana Pipiens. Q. J. Exp. Physiol.* 63:301–314.

Chávez, E., C. Bravo, and J.A. Holguín. 1987. Metabolite transport in mitochondria as a function of osmolarity. *Arch. Biochem. Biophys.* 253:94–99.

Chinet, A. 1993. Ca^{2+}-dependent heat production by rat skeletal muscle in hypertonic media depends on Na^+-Cl^- co-transport stimulation. *J. Physiol. (Lond.).* 461:689–703.

Chinet, A., and P. Giovannini. 1989. Evidence by calorimetry for an activation of sodium-hydrogen exchange of young rat skeletal muscle in hypertonic media. *J. Physiol. (Lond.).* 415:409–422.

Clausen, T. 1968. The relationship between the transport of glucose and cations across cell membranes in isolated tissues. III. Effect of Na^+ and hyperosmolarity on glucose metabolism and insulin responsiveness in isolated rat hemidiaphragm. *Biochim. Biophys. Acta.* 150:56–65.

Clausen, T., A.B. Dahl-Hansen, and J. Elbrink. 1979. The effect of hyperosmolarity and insulin on resting tension and calcium fluxes in rat soleus muscle. *J. Physiol. (Lond.).* 292:505–526.

Clausen, T., J. Gliemann, J. Vinten, and P.G. Kohn. 1970. Stimulating effect of hyperosmolarity on glucose transport in adipocytes and muscle cells. *Biochim. Biophys. Acta.* 211:233–243.

Coronado, R., J. Morrissette, M. Sukhareva, and D.M. Vaughan. 1994. Structure and function of ryanodine receptors. *Am. J. Physiol.* 266:C1485–C1504.

Daemers-Lambert, C., F.-M. Debrun, G. Dethier, and J. Manil. 1966. Métabolisme des esters phosphorés dans le sartorius de *Rana temporaria* traité par une solution de Ringer hypertonique. *Arch. Int. Physiol. Biochim.* 74:374–396.

Dale, H.H. 1913. The effect of small variations in concentration of Ringer's solution on the response of isolated plain muscle. *J. Physiol. (Lond.).* 46:XIX.

Daut, J., and G. Elzinga. 1988. Heat production of quiescent ventricular trabeculae isolated from guinea-pig heart. *J. Physiol. (Lond.).* 398:259–275.

de Beer, E.L., R.L.F. Grundeman, A.J. Wilhelm, C. van den Berg, C.J. Canjouw, D. Klepper, and P. Schiereck. 1988. Effect of sarcomere length and filament lattice spacing on force development in skinned cardiac and skeletal muscle preparations from the rabbit. *Basic Res. Cardiol.* 83:410–423.

Demoor, M.J., and M. Philippson. 1908. Influence de la pression osmotique sur l'allure de la contraction musculaire. *Bulletin de l'Academie Royalé de Médecin de Belgique.* XXII:655–667.

Ebus, J.P., and G.J.M. Stienen. 1996. Origin of concurrent ATPase activities in skinned cardiac trabeculae from rat. *J. Physiol. (Lond.).* 492:675–687.

Edman, K.A.P., and J.C. Hwang. 1977. The force-velocity relationship in vertebrate muscle fibres at varied tonicity of the extracellular medium. *J. Physiol. (Lond.).* 269:255–272.

Erac, I.E., P.J. Cooper, P.J. Hanley, and D.S. Loiselle. 1996. Effects of hyperosmolarity on mechanical performance of isolated rat cardiac trabeculae. *Proc. Physiol. Soc. New Zealand.* 15:In press.

Fiolet, J.W.T., A. Baartscheer, and C.A. Schumacher. 1995. Intracellular $[Ca^{2+}]$ and VO_2 after manipulation of the free-energy of the Na^+/Ca^{2+}-exchanger in isolated rat ventricular myocytes. *J. Mol. Cell. Cardiol.* 27:1513–1525.

Ford, L.E., K. Nakagawa, J. Desper, and C.Y. Seow. 1991. Effect of osmotic compression on the force-velocity properties of glycerinated rabbit skeletal muscle cells. *J. Gen. Physiol.* 97:73–88.

Fortune, N.S., M.A. Geeves, and K.W. Ranatunga. 1994. Contractile activation and force generation in skinned rabbit muscle fibres: effects of hydrostatic pressure. *J. Physiol. (Lond.).* 474:283–290.

Goldman, Y.E., and R.M. Simmons. 1986. The stiffness of frog

skinned muscle fibres at altered lateral filament spacing. *J. Physiol. (Lond.).* 378:175–194.

Grynkiewicz, G., M. Poenie, and R.Y. Tsien. 1985. A new generation of Ca^{2+} indicators with greatly improved fluorescence properties. *J. Biol. Chem.* 260:3440–3450.

Gulati, J., and A. Babu. 1984. Intrinsic shortening speed of temperature-jump-activated intact muscle fibers. Effects of varying osmotic pressure with sucrose and KCl. *Biophys. J.* 45:431–445.

Halestrap, A.P. 1989. The regulation of the matrix volume of mammalian mitochondria in vivo and in vitro and its role in the control of mitochondrial metabolism. *Biochim. Biophys. Acta.* 973: 355–382.

Hanley, P.J., P.J. Cooper, and D.S. Loiselle. 1994*a*. Effect of hyperosmotic perfusion on rate of oxygen consumption of isolated guinea pig and rat hearts during cardioplegia. *Cardiovasc. Res.* 28: 285–493.

Hanley, P.J., P.J. Cooper, and D.S. Loiselle. 1994*b*. Energetic effects of caffeine in face of retarded Na^+/Ca^{2+} exchange in isolated, arrested guinea pig hearts. *Am. J. Physiol.* 267:H1663–H1669.

Hermsmeyer, K., R. Rulon, and N. Sperelakis. 1972. Loss of the plateau of the cardiac action potential in hypertonic solutions. *J. Gen. Physiol.* 59:779–793.

Hill, A.V. 1965. Trails and Trials in Physiology. Edward Arnold Ltd., London. 374 pp.

Hill, D.K. 1968. Tension due to interaction between the sliding filaments in resting striated muscle. The effect of stimulation. *J. Physiol. (Lond.).* 199:637–684.

Hirvonen, L. 1955. Electrographic studies of the isolated rabbit auricle. *Ann. Med. Exp. Biol. Fenn.* 33:1–96.

Homsher, E., F.N. Briggs, and R.M. Wise. 1974. Effects of hypertonicity on resting and contracting frog skeletal muscles. *Am. J. Physiol.* 226:855–863.

Kawai, M., J.S. Wray, and K. Güth. 1990. Effect of ionic strength on crossbridge kinetics as studied by sinusoidal analysis, ATP hydrolysis rate and X-ray diffraction techniques in chemically skinned rabbit psoas fibres. *J. Musc. Res. Cell Motil.* 11:392–402.

Kawata, H., and K. Kawagoe. 1975. Effects of tonicity on the resting tension in bullfrog ventricle. *Jpn. J. Physiol.* 25:65–78.

Kawata, H., M. Ohba, J. Hatae, and M. Kishi. 1983. A study on the mechanism of twitch potentiation by hypertonic solution in the frog atrial muscle. *J. Mol. Cell. Cardiol.* 15:281–293.

Kent, R.L., R.J. Sheldon, and C. Harakal. 1983. The effects of hyperosmolar solutions on isolated vascular smooth muscle examined with verapamil. *Pharmacology.* 26:157–163.

Kentish, J.C. 1984. The inhibitory effects of monovalent ions on force development in detergent-skinned ventricular muscle from guinea-pig. *J. Physiol. (Lond.).* 352:353–374.

Koch-Weser, J. 1963. Influence of osmolarity of perfusate on contractility of mammalian myocardium. *Am. J. Physiol.* 204:957–962.

Krasner, B., and D. Maughan. 1984. The relationship between ATP hydrolysis and active force in compressed and swollen skinned muscle fibers of the rabbit. *Pflüg. Arch.* 400:160–165.

Kuzuya, T., E. Samols, and R.H. Williams. 1965. Stimulation by hyperosmolarity of glucose metabolism in rat adipose tissue and diaphragm in vitro. *J. Biol. Chem.* 240:2277–2283.

Lado, M.G., S.-S. Sheu, and H.A. Fozzard. 1984. Effects of tonicity on tension and intracellular sodium and calcium activities in sheep heart. *Circ. Res.* 54:576–585.

Lamb, G.D., D.G. Stephenson, and G.J.M. Stienen. 1993. Effects of osmolality and ionic strength on the mechanism of Ca^{2+} release in skinned skeletal muscle fibres of the toad. *J. Physiol. (Lond.).* 464:629–648.

Lännergren, J. 1971. The effect of low-level activation on the mechanical properties of isolated frog muscle fibers. *J. Gen. Physiol.* 58:145–162.

Lännergren, J., and J. Noth. 1973. Tension in isolated frog muscle fibers induced by hypertonic solutions. *J. Gen. Physiol.* 61:158–175.

Little, G.R., and W.W. Sleator. 1969. Calcium exchange and contraction strength of guinea pig atrium in normal and hypertonic media. *J. Gen. Physiol.* 54:494–511.

Loiselle, D.S. 1987. Cardiac basal and activation metabolism. *Basic Res. Cardiol.* 82:37–50.

Månsson, A. 1994. The tension response to stretch of intact skeletal muscle fibres of the frog at varied tonicity of the extracellular medium. *J. Musc. Res. Cell Motil.* 15:145–157.

Martonosi, A., and R. Feretos. 1964. Sarcoplasmic reticulum. II. Correlation between adenosine triphosphatase activity and Ca^{++} uptake. *J. Biol. Chem.* 239:659–668.

Matsubara, I., Y.E. Goldman, and R.M. Simmons. 1984. Changes in the lateral filament spacing of skinned muscle fibres when crossbridges attach. *J. Mol. Biol.* 173:15–33.

Metzger, J.M., and R.L. Moss. 1987. Shortening velocity in skinned single muscle fibers: influence of filament lattice spacing. *Biophys. J.* 52:127–131.

Miyata, H., H.S. Silverman, S.J. Sollott, E.G., Lakatta, M.D. Stern, and R.G. Hansford. 1991. Measurement of mitochondrial free Ca^{2+} concentration in living single rat cardiac myocytes. *Am. J. Physiol.* 261:H1123–H1134.

Nicholls, D.G., H.J. Grav, and O. Lindberg. 1972. Mitochondria from hamster brown-adipose tissue: regulation of respiration *in vitro* by variations in volume of the matrix compartment. *Eur. J. Biochem.* 31:526–533.

Ogawa, Y., and H. Harafuji. 1990. Osmolarity-dependent characteristics of [^{3}H]ryanodine binding to sarcoplasmic reticulum. *J. Biochem.* 107:894–898.

Ohba, M. 1984. A role of ionic strength on the inotropic effects of osmolarity change in frog atrium. *Jpn. J. Physiol.* 34:1105–1115.

Omachi, A., R.A. Kleps, T.O. Henderson, and R.J. Labotka. 1994. Inhibition of the calcium paradox in isolated rat hearts by high perfusate sucrose concentrations. *Am. J. Physiol.* 266:H1729–H1737.

Overton, E. 1902. Beiträge zur allgemeinen muskel- und nervenphysiologie. *Pflüg. Archiv.* 92:115–280.

Ponce-Hornos, J.E. 1989. Heart energetics: a framework for ion flux analysis. *J. Mol. Cell. Cardiol.* 21:115–117.

Rapoport, S.I., V. Nassar-Gentina, and J.V. Passoneau. 1982. Effects of excitation-contraction uncoupling by stretch and hypertonicity on metabolism and tension in single frog muscle fibers. *J. Gen. Physiol.* 80:73–81.

Schramm, M., H.-G. Klieber, and J. Daut. 1994. The energy expenditure of actomyosin-ATPase, Ca^{2+}-ATPase and Na^+,K^+-ATPase in guinea-pig cardiac ventricular muscle. *J. Physiol. (Lond.).* 481: 647–662.

Sekine, T., J. Iijima, T. Genba, K. Tanaka, and M. Kanai. 1957. About the increase of respiration during the muscle activity. *In* Conference on the Chemistry of Muscular Contraction. Igaka Shoin, Tokyo. 1958 pp.

Slater, E.C., and K.W. Cleland. 1953. The effect of tonicity of the medium on the respiratory and phosphorylative activity of heart-muscle sarcosomes. *Biochemistry.* 53:557–567.

Sperelakis, N., T. Hoshiko, R.F. Keller, and R.M. Berne. 1960. Intracellular and external recording from frog ventricular fibers during hypertonic perfusion. *Am. J. Physiol.* 198:135–140.

Sperelakis, N., and R. Rubio. 1971. Ultrastructural changes produced by hypertonicity in cat cardiac muscle. *J. Mol. Cell. Cardiol.* 3:139–156.

Tsuchiya, T. 1988. Passive interaction between sliding filaments in the osmotically compressed skinned muscle fibers of the frog. *Biophys. J.* 53:415–423.

Uto, A., H. Arai, and Y. Ogawa. 1991. Reassessment of Fura-2 and the ratio method for determination of intracellular Ca^{2+} concentrations. *Cell Calcium.* 12:29–37.

van Hardeveld, C., V.J.A. Schouten, A. Muller, E.T. van der Meulen, and G. Elzinga. 1995. Exposure of energy-depleted rat trabeculae to low pH improves contractile recovery: role of calcium. *Am. J. Physiol.* 268:H1510–H1520.

Vornanen, M. 1987. Effects of procaine and caffeine on the contractility of enzymatically isolated myocytes and intact cardiac tissue. *Gen. Pharmacol.* 18:599–604.

Whalley, D.W., P.D. Hemsworth, and H.H. Rasmussen. 1994. Regulation of intracellular pH in cardiac muscle during cell shrinkage and swelling in anisosmolar solutions. *Am. J. Physiol.* 266:H658–H669.

Whalley, D.W., L.C. Hool, R.E. ten Eick, and H.H. Rasmussen. 1993. Effect of osmotic swelling and shrinkage on Na^+-K^+ pump activity in mammalian cardiac myocytes. *Am. J. Physiol.* 265: C1201–C1210.

Willerson, J.T., S. Wheelan, R.C. Adcock, G.H. Templeton, and K. Wildenthal. 1978. Species differences in responses to hyperosmolality and D600 in cat and rat heart. *Am. J. Physiol.* 235:H276–H280.

Yamada, K. 1970. The increase in the rate of heat production of frog's skeletal muscle caused by hypertonic solutions. *J. Physiol. (Lond.).* 208:49–64.

Zhao, Y., and M. Kawai. 1993. The effect of the lattice spacing change on cross-bridge kinetics in chemically skinned rabbit psoas muscle fibers. II. Elementary steps affected by the spacing change. *Biophys. J.* 64:197–210.